

Supporting Information

Synthesis and electron-transport properties of *N*-trifluoromethylphenyl-phthalimides containing selenophene substituents

Jun-ichi Nishida,^{a*} Yoshiki Morikawa,^a Akito Hashimoto,^a Yasuyuki Kita,^a Hiroshi Nishimoto,^a Tomofumi Kadoya,^b Hiroyasu Sato,^b Takeshi Kawase^a

^a Department of Applied Chemistry, Graduate School of Engineering, University of Hyogo, 2167 Shosha, Himeji, Hyogo 671-2280, Japan

^b Department of Material Science, Graduate School of Science, University of Hyogo, 3-2-1 Kouto, Kamigori-cho, Ako-gun, Hyogo 678-1297, Japan

^c Rigaku Corporation, 3-9-12 Matsubaracho, Akishima, Tokyo 196-8666, Japan

E-mail: jnishida@eng.u-hyogo.ac.jp

Contents	p. 1
1. Synthesis of materials	p. 2
2. X-ray crystal structure analysis	p. 5
3. UV-Vis absorption spectra in solution	p. 7
4. Photoluminescence spectra in solution	p. 7
5. Diffuse reflectance spectra in solids.	p. 8
6. Absorption spectra in thin films.	p. 9
7. XRD patterns	p. 10
8. Redox properties	p. 12
9. Redox properties in thin films	p. 13
10. FET measurements with LED	p. 14
11. LED used in the measurements	p. 15
12. FET characteristics	p. 17
13. Conductivity	p. 19
14. FET made by raiging substrate to 100 °C during deposition	p. 20
15. Change of FET output characteristics depending on I_{LED}	p. 22
16. Changes of FET transfer characteristics depending on I_{LED}	p. 23
17. Molecular orbitals and TD-DFT calculations	p. 24
18. Overlap integrals of biselenophene derivative 2 and bithiophene derivative 2T	p. 32
19. ¹ H-NMR data.	p. 33
20. ¹³ C-NMR data.	p. 35
21. IR data (KBr pellet).	p. 36

1, Synthesis of materials

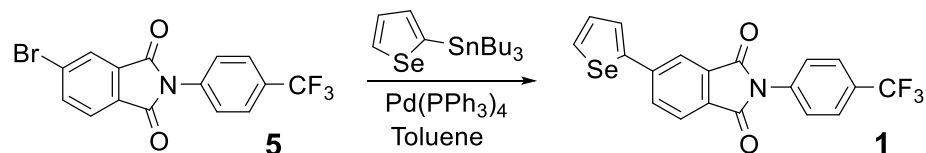
General Procedure.

Tetrakis(triphenylphosphine)palladium(0): Pd(PPh₃)₄, *n*-butyllithium in *n*-hexane, tributyltin chloride, 5-bromo-isobenzofuran-1,3-dione (4-bromophthalic anhydride), 4-(trifluoromethyl)aniline, *N*-bromosuccinimide (NBS) and DMF were purchased and used without further purification. NMR spectrometers and the chemical shifts were referenced to tetramethylsilane (TMS). Photoluminescence (PL) quantum yields in the solid state were determined by using an integrating sphere. Cyclic voltammograms were measured by using a Pt disk working electrode, a Pt wire counter, and Ag/Ag⁺ reference electrode. Tetrabutylammonium hexafluorophosphate (TBAPF₆: 0.1 mol dm⁻³) was used as a supporting electrolyte in dry DMF.

Synthesis of 5-(Selenophen-2-yl)-2-(4-trifluoromethylphenyl)-isoindole-1,3-dione (PI 1)

A mixture of bromo substituted PI **5** (1.77 g, 4.77 mmol), 2-(tributylstannylyl)selenophene (3.01 g, 7.17 mmol), Pd(PPh₃)₄ (62.8 mg, 0.0540 mmol) in dry toluene (30 ml) was refluxed under N₂ for 24 hr. After cooling to RT, solvent was evaporated. The resulting solid was triturated with MeOH and collected by suction. Purification by sublimation gave a pale yellow solid of selenophene substituted phthalimide (PI) **5** (1.60 g, 80%).

Mp 266–267 °C. ¹H NMR (CDCl₃, 400 MHz, 20 °C): δ 8.16–8.13 (m, 2H), 7.99–9.93 (m, 2H), 7.79 (d, *J* = 8.6 Hz, 2H), 7.72 (dd, *J* = 3.6, 0.8 Hz, 1H), 7.66 (d, *J* = 8.6 Hz, 2H), 7.42 (dd, *J* = 5.6, 3.6 Hz, 1H). ¹³C NMR (100 MHz, CDCl₃, 20 °C) δ = 166.6 (C=O), 166.4 (C=O), 147.8, 143.2, 134.9, 133.3, 132.6, 131.9, 131.2, 129.8 (quartet, *J* = 33.5 Hz, C(Ph)-CF₃), 129.4, 128.2, 126.4 (2C), 126.3 (2C), 124.7, 123.8 (quartet, *J* = 270 Hz, CF₃), 121.1. IR(KBr) ν max/cm⁻¹ 3070, 1717, 1614, 1399, 1338, 1117, 1069, 836, 698. MS(EI⁺, 70 eV) *m/z* (rel. intensity) = 421([M]⁺, 100), 419([M-2]⁺, 50), 377(52). HRMS (EI⁺): *m/z* calcd for C₁₉H₁₀F₃NO₂Se: 420.9829 [M⁺]; found: 420.9826.

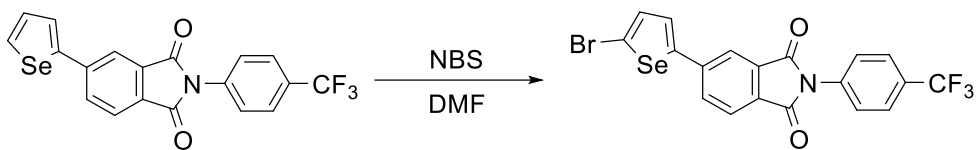


Synthesis of 5-(5-Bromoselenophen-2-yl)-2-(4-trifluoromethylphenyl)-isoindole-1,3-dione (PI 6)

A mixture of selenophene substituted PI **1** (502 mg, 1.19 mmol) and NBS (218 mg, 1.23 mmol) in DMF (8 mL) was stirred at 70 °C under N₂ for 24 hr. After cooling to RT, the reaction mixture was poured into ice bath. The resulting yellow precipitates was collected by suction and washed with methanol. An yellowish-orange solid of bromine substituted PI **6** (553 mg) was obtained in 93% yield.

Mp 244–245 °C. ¹H NMR (CDCl₃, 400 MHz, 20 °C): δ 8.04 (d, *J* = 1.2 Hz, 1H), 7.96 (d, *J* = 7.8 Hz, 1H), 7.85 (dd, *J* = 7.8, 1.2 Hz, 1H), 7.79 (d, *J* = 8.8 Hz, 2H), 7.65 (d, *J* = 8.8 Hz, 2H), 7.41 (d, *J* = 4.0 Hz, 1H), 7.35 (d, *J* = 4.0 Hz, 1H). ¹³C NMR (100 MHz, CDCl₃, 20 °C) δ = 166.4 (C=O), 166.3 (C=O), 149.3, 142.3, 134.8, 134.6, 132.7, 131.6, 129.9 (quartet, *J* = 37.3 Hz, C(Ph)-CF₃), 129.7, 128.1, 126.4 (2C), 126.3 (2C), 124.9, 123.8 (quartet, *J* = 270 Hz, CF₃), 120.7, 118.4. IR(KBr) ν max/cm⁻¹ 3063, 1779, 1712, 1614, 1385, 1323, 1132, 1065, 840, 743. MS(EI) *m/z* (rel. intensity) =

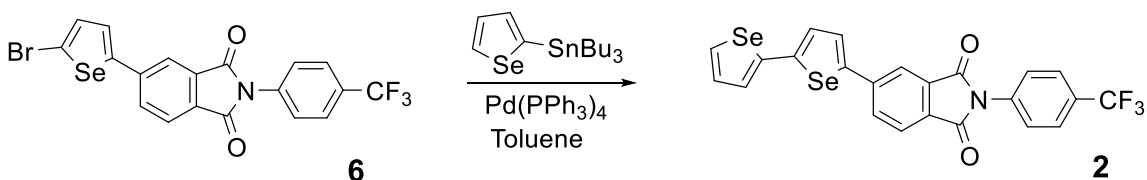
499([M]⁺,100), 501([M+2]⁺,78), 497([M-2]⁺,45). HRMS (EI⁺): *m/z* calcd for C₁₉H₉BrF₃NO₂Se: 498.8934 [M⁺]; found: 498.8940.



Synthesis of 5-(2,2'-biselenophen-5-yl)-2-(4-trifluoromethylphenyl)-isoindole-1,3-dione (PI 2)

A mixture of bromine substituted PI **6** (510 mg, 1.02 mmol) and 2-tributylstannylselenophene (658 mg, 1.57 mmol), Pd(PPh₃)₄ (84.6 mg, 0.0730 mmol) in dry toluene (20 mL) was reflux under N₂ for 24 hr. After cooling to RT, the solvent was removed. The residue was triturated with methanol, and the resulting solid was collected by suction and washed with methanol. Purification by sublimation gave a yellowish-orange solid of PI **2** (334 mg, 60%).

Mp >300 °C. ¹H NMR (CDCl₃, 400 MHz, 20 °C): δ 8.10 (br. s, 1H), 7.98-7.90 (m, 3H), 7.79 (d, *J* = 8.8 Hz, 2H), 7.66 (d, *J* = 8.8 Hz, 2H), 7.63 (d, *J* = 4.2 Hz, 1H), 7.36 (br. d, *J* = 3.6 Hz, 1H), 7.32 (d, *J* = 4.2 Hz, 1H), 7.29-7.25 (m, 1H). IR(KBr) *v* max/cm⁻¹ 3066, 1785, 1718, 1614, 1432, 1397, 1338, 1120, 1069, 832. MS(EI) *m/z* (rel. intensity) = 551([M]⁺,100), 549([M-2]⁺,92), 547([M-4]⁺,53). HRMS (EI⁺): *m/z* calcd for C₂₃H₁₂F₃NO₂Se₂: 550.9151 [M⁺]; found: 550.9155. Anal. Calcd for C₂₃H₁₂F₃NO₂Se₂: C, 50.29; H, 2.20; N, 2.55. Found: C, 50.26; H, 2.10; N, 2.48. ¹³C-NMR could not be measured because of low solubility.

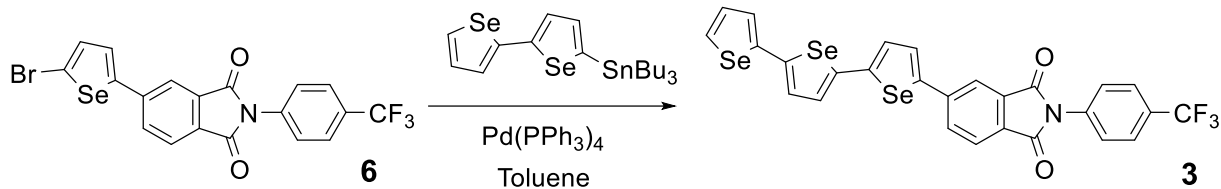


Synthesis of 5-(2,2'-biselenophen-5-yl)-2-(4-trifluoromethylphenyl)-isoindole-1,3-dione (PI 3)

To a solution of 5-bromo-2,2'-biselenophene in THF (5 ml) was added *n*-BuLi in hexane solution (0.700 ml, 1.05 mol) for 1 min at -78 °C under N₂ and the solution was stirred for 30 min. To the solution was added tributyltin chloride (290 mg, 0.890 mmol) for 1 min, and the solution was stirred for 1 hr at -78 °C. The reaction mixture was slowly warmed to room temperature and stirred for 1 hr. The reaction mixture was diluted with hexane and poured into a saturated NaHCO₃ aqueous solution. Organic layer was washed with brine and dried over Na₂SO₄. After evaporation of solvent, 5-tributylstannyl-2,2'-biselenophene was obtained as brown oil (372 mg, 86%). This oil was used in the next reaction without further purification.

A mixture of bromine substituted PI **6** (226 mg, 0.450 mmol) and 5-tributylstannyl-2,2'-biselenophene (372 mg, 0.680 mmol), Pd(PPh₃)₄ (23.9 mg, 0.0210 mmol), in dry toluene (10 mL) was reflux for 22 hr. After cooling to RT, the solvent was removed. The residue was triturated with methanol, and the resulting solid was collected by suction and washed with methanol. Purification by sublimation gave reddish-brown solid of PI **3** (138 mg, 0.200 mmol) in 45% yield.

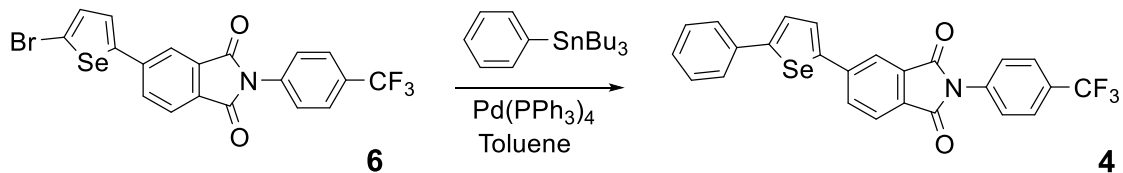
Mp >300 °C. IR(KBr) *v* max/cm⁻¹ 3049, 1783, 1717, 1614, 1372, 1333, 1121, 1068, 837, 793. MS(EI⁺) *m/z* (rel. intensity) = 679([M]⁺,100), 681([M+2]⁺,83), 677([M-2]⁺, 77). HRMS (EI⁺): *m/z* calcd for C₂₇H₁₄F₃NO₂Se₃: 680.8472 [M⁺]; found: 680.8483. Anal. Calcd for C₂₇H₁₄F₃NO₂Se₃: C, 47.81; H, 2.08; N, 2.06. Found: C, 48.10; H, 2.17; N, 2.06. ¹H NMR and ¹³C-NMR could not be measured because of low solubility.



Synthesis of 5-(5-phenylselenophen-2-yl)-2-(4-trifluoromethylphenyl)-isoindole-1,3-dione (PI 4)

A mixture of bromo substituted PI **6** (505 mg, 1.01 mmol) and tributylstannylnbenzene (635 mg, 1.73 mmol), Pd(PPh₃)₄ (74.8 mg, 0.065 mmol), in dry toluene (20 mL) was reflux for 24 hr under N₂. After cooling to RT, the solvent was removed. The residue was triturated with methanol, and the resulting solid was collected by suction and washed with methanol. Purification by sublimation gave yellow solid of PI **4** (316 mg, 63%).

Mp >300 °C. ¹H NMR (CDCl₃, 400MHz): δ 8.14 (s, 1H), 7.98-7.96 (m, 2H), 7.80 (d, *J* = 8.2 Hz, 2H), 7.72 (d, *J* = 4.4 Hz, 1H), 7.66 (d, *J* = 8.2 Hz, 2H), 7.61 (br. d, *J* = 7.2 Hz, 2H), 7.54 (d, *J* = 4.4 Hz, 1H), 7.45-7.40 (m, 2H), 7.36 (br. t, *J* = 6.8 Hz, 1H). IR(KBr) ν max/cm⁻¹ 3066, 1784, 1716, 1614, 1399, 1338, 1119, 1070, 836, 754. MS(EI⁺) *m/z* (rel. intensity) = 497([M]⁺,100), 495([M-2]⁺,52). HRMS (EI⁺): *m/z* calcd for C₂₅H₁₄F₃NO₂Se: 680.8472 [M⁺]; found: 680.8483. Anal. Calcd for C₂₅H₁₄F₃NO₂Se: C, 60.50; H, 2.84; N, 2.82. Found: C, 60.25; H, 2.89; N 2.83. ¹³C-NMR could not be measured because of low solubility.



2. X-ray crystal structure analysis

X-ray measurements of single crystals of **2** were made on a Rigaku XtaLAB Synergy-Custom, four-circle diffractometer using Cu-K α radiation ($\lambda = 1.54184 \text{ \AA}$) at 93 K, and all calculations were performed using CrysAlisPro (Rigaku Oxford Diffraction, 2020). The structures were solved by direct methods (ShelXT : Sheldrick, 2015)¹ and were refined by full-matrix least-squares on all unique F^2 values (SHELXL 2018/3 : Sheldrick, 2015)², interfaced through the program OLEX2³, with anisotropic displacement parameters for all non-hydrogen atoms, and with constrained riding hydrogen geometries. Empirical absorption corrections were applied using spherical harmonics, implemented in SCALE3 ABSPACK scaling algorithm. Some disorder refinements were done using SIMU, RIGU and SADI.

Crystal data for **2**: an orange plate crystal, $C_{23}H_{12}F_3NO_2Se_2$, $M = 549.26$, crystal dimensions $0.077 \times 0.034 \times 0.008 \text{ mm}$, monoclinic, space group Pn , $a = 5.77820(14)$, $b = 7.8504(2)$, $c = 42.3511(12) \text{ \AA}$, $\beta = 91.026(3)$, $V = 1920.80(9) \text{ \AA}^3$, $Z = 4$, $D_c = 1.899 \text{ g cm}^{-3}$, 23086 reflections collected, 6272 independent ($R_{int} = 0.0320$), GOF = 1.051, $R_1 [F^2 > 2\sigma(F^2)] = 0.0339$, and $wR_2(F^2) = 0.0921$ for all reflections. Flack parameter 0.019(14). CCDC number is 2101621.

1 G. M. Sheldrick, *Acta Cryst.*, 2015, **A71**, 3–8.

2 G. M. Sheldrick, *Acta Cryst.*, 2015, **C71**, 3–8.

3 O. V. Dolomanov, L. J. Bourhis, R. J. Gildea, J. A. K. Howard, and H. Puschmann, *J. Appl. Cryst.* 2009, **42**, 339–341.

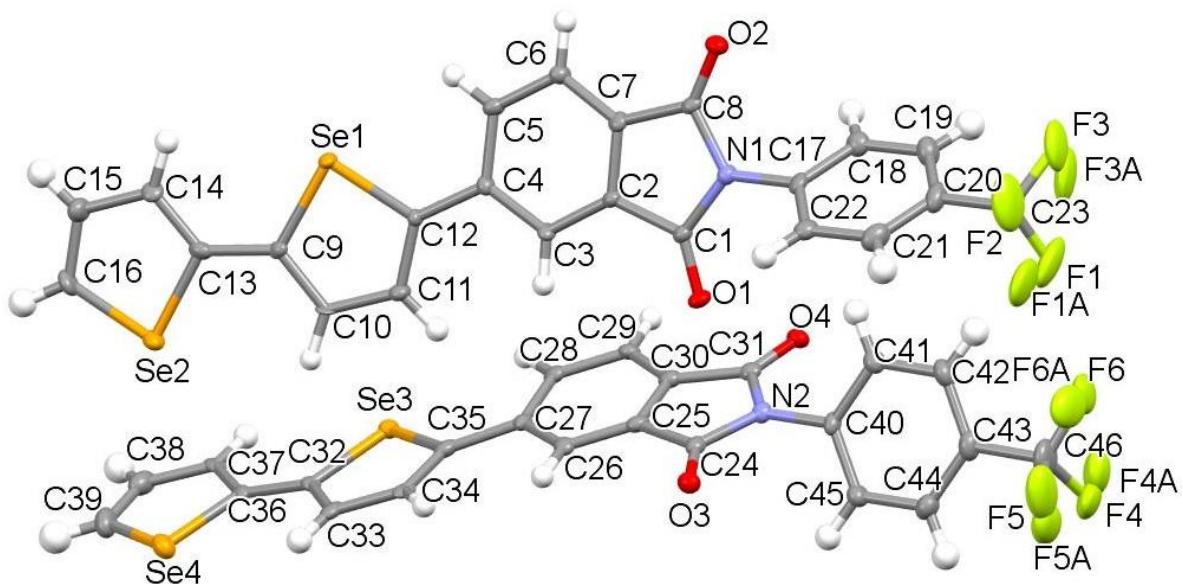


Fig. S1 Molecular structures of PI derivative **2** (50% probability).

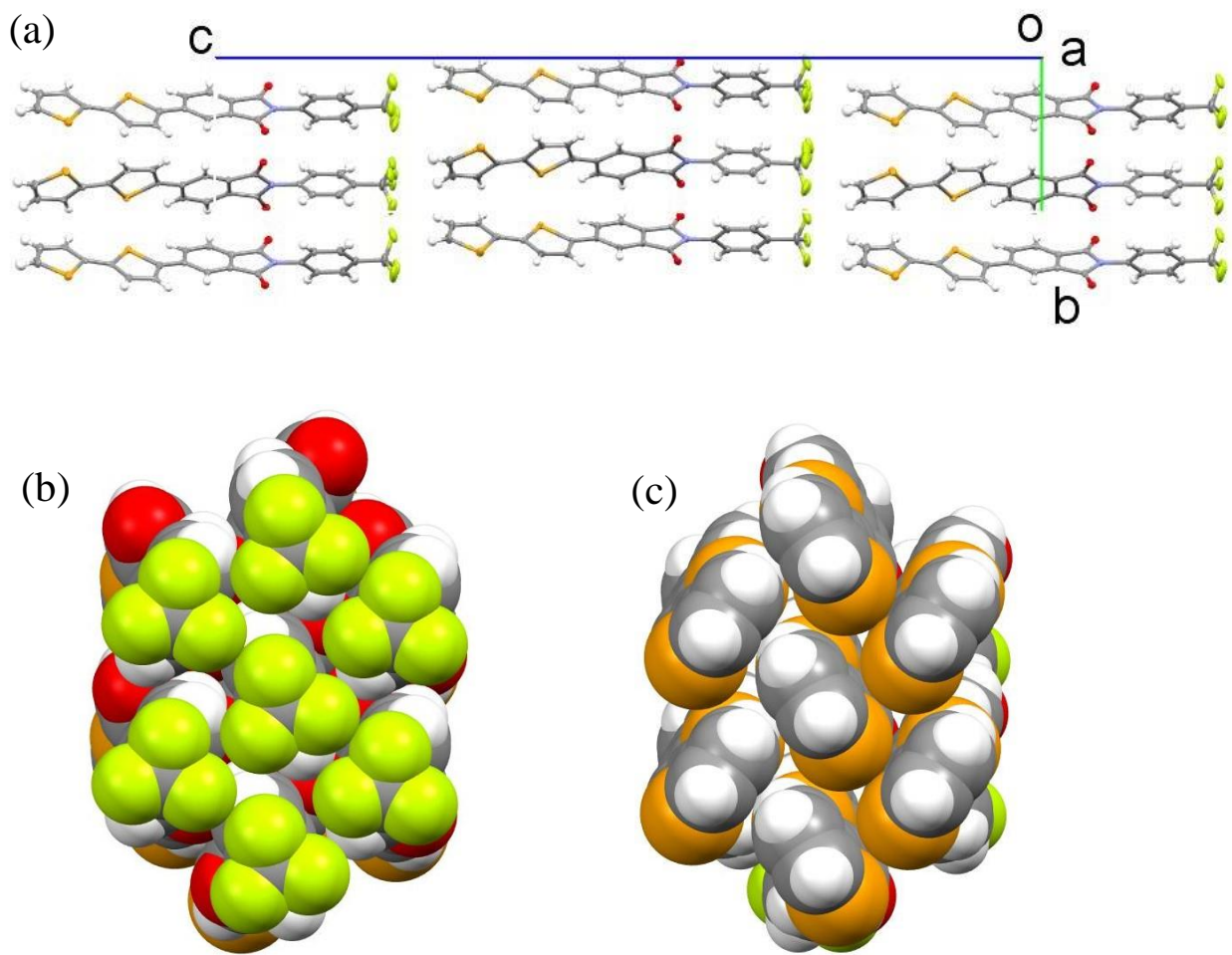


Fig. S2 (a) Crystal packing of **2** viewed along **a**-axis. (b) Close atom contacts viewed from trifluoromethylphenyl group side. (c) Close atom contacts viewed from selenophene units.

3. UV-Vis absorption spectra in solution

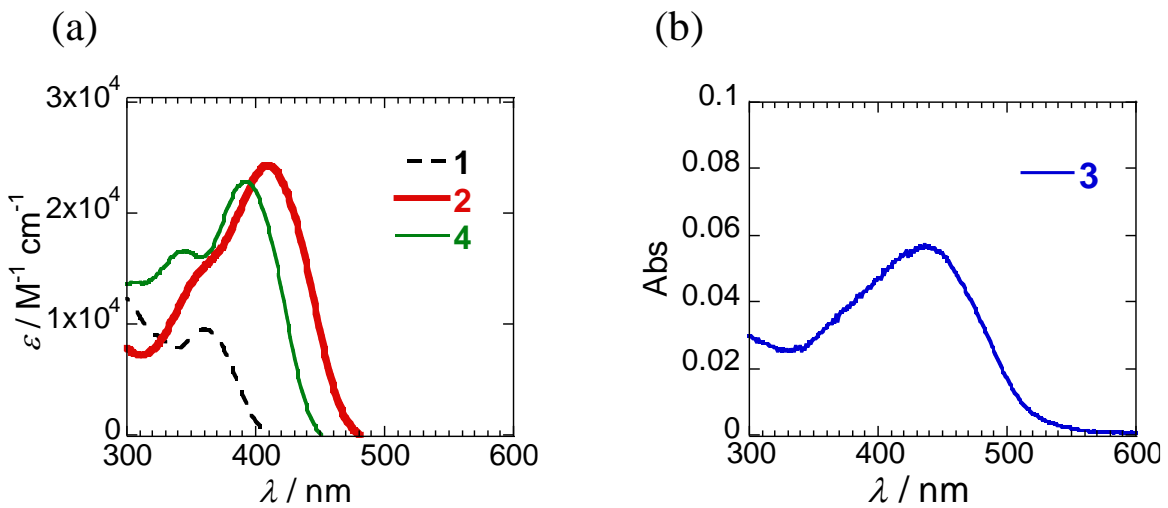


Fig. S3 Absorption spectra of PI derivatives (a) **1,2,4** and (b) **3** in dichloromethane (DCM).

4. Photoluminescence spectra in solution

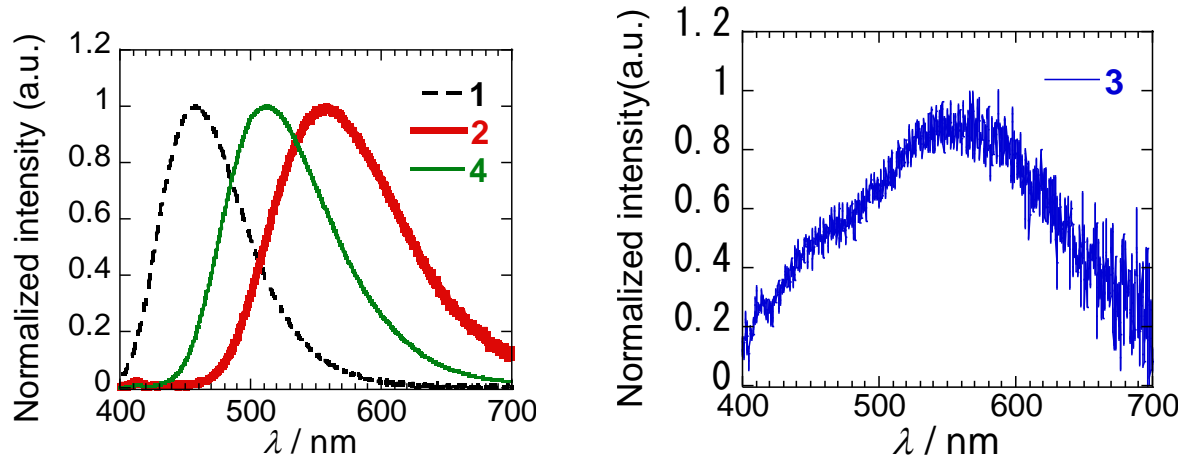
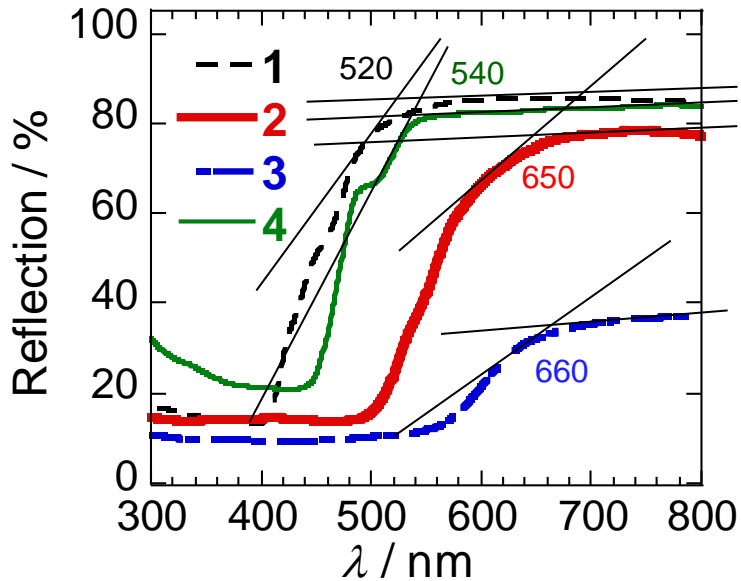


Fig. S4 PL spectra of PI derivatives (a) **1,2,4** and (b) **3** in DCM ($\lambda_{\text{ex}} = 366 \text{ nm}$).

5. Diffuse reflectance spectra in solids

(a)



(b)

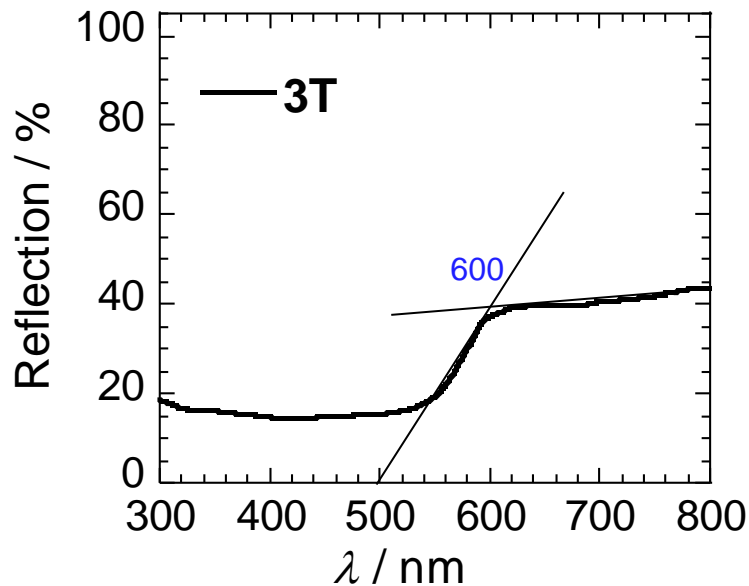


Fig. S5 Diffuse reflectance spectra in solids of (a) 1–4 and (b) 3T.

6. Absorption spectra in thin films

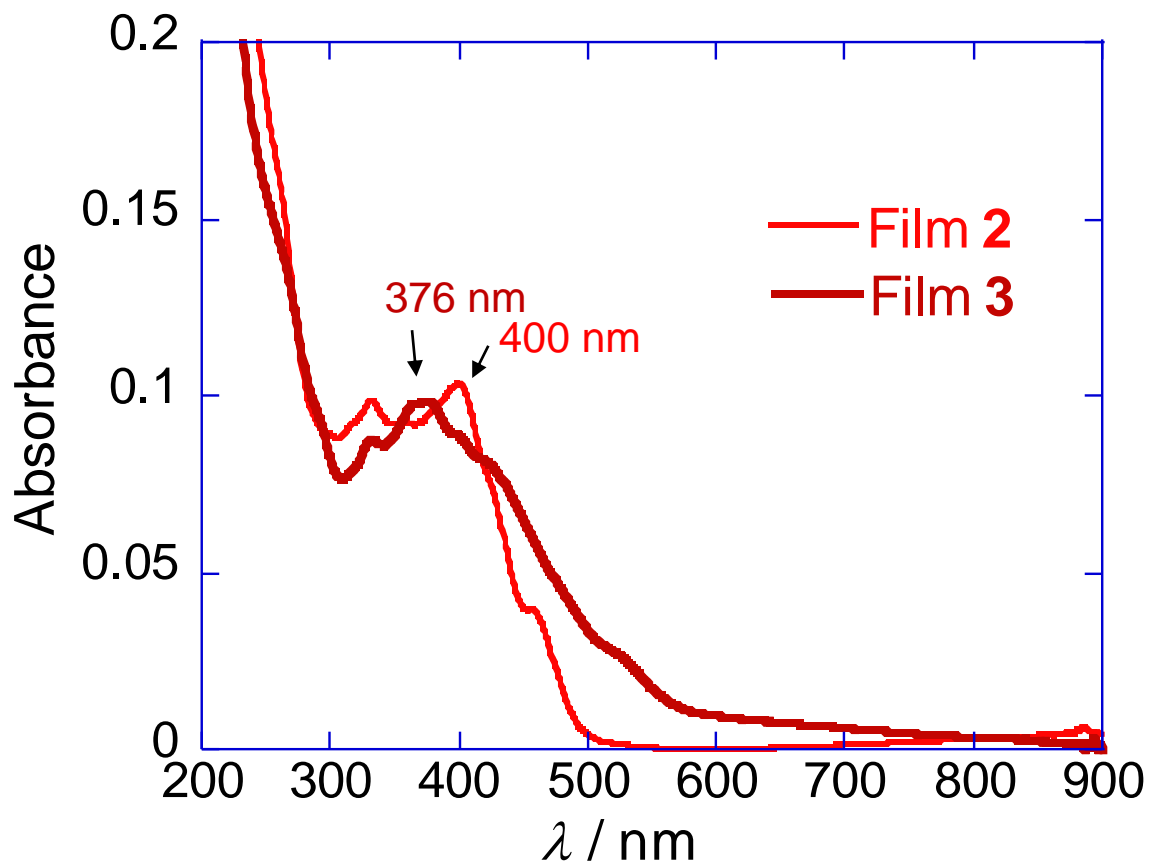


Fig. S6 UV-Vis spectra of thin films of **2** and **3** (60 nm) deposited on quartz glass.

7. XRD patterns

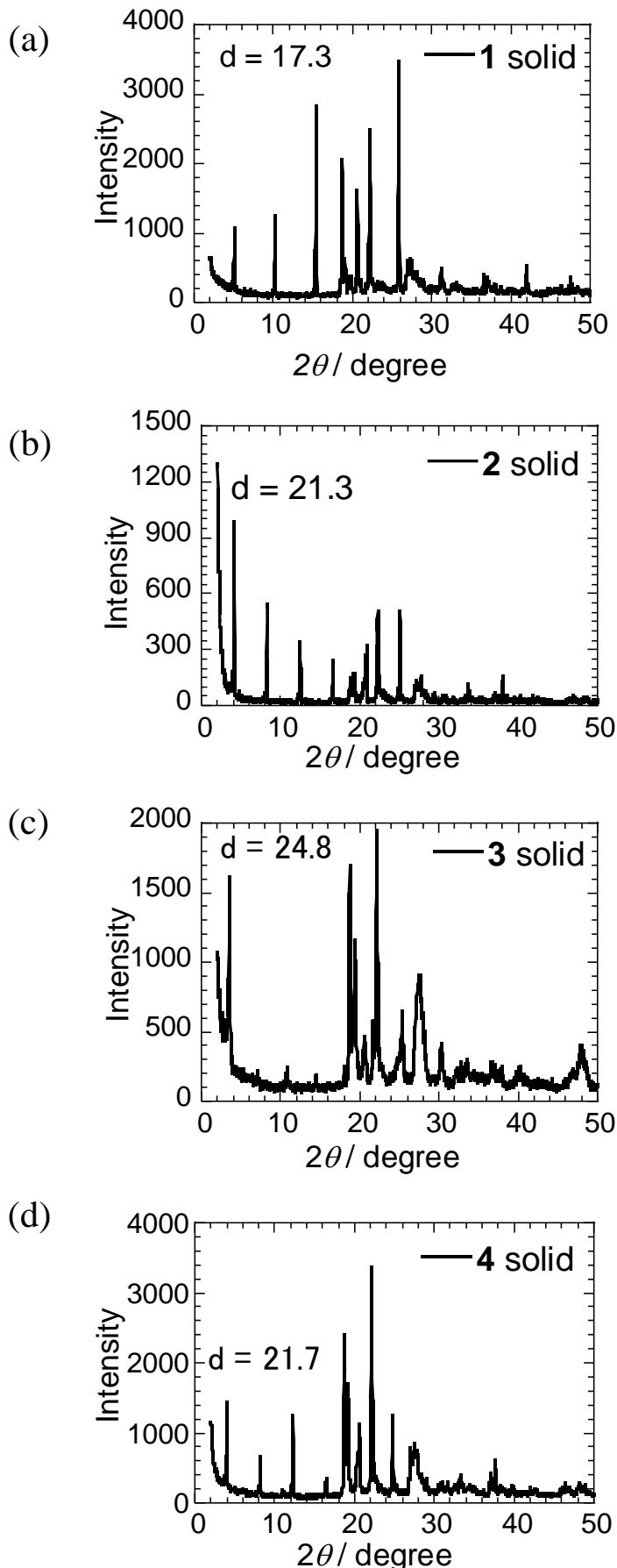
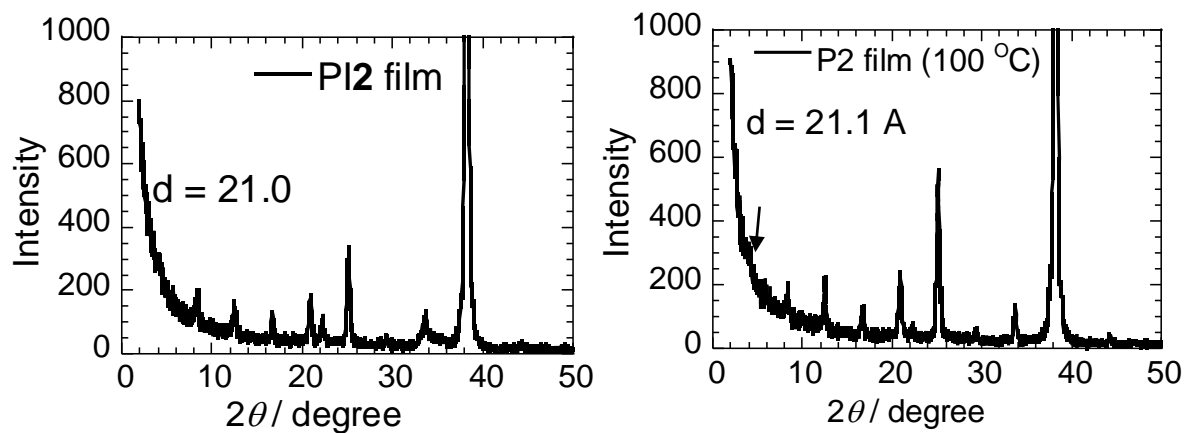
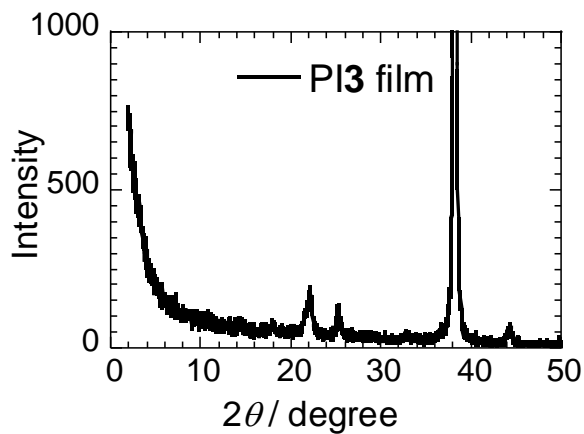


Fig. S7A XRD patterns of (a) powder **1**, (b) powder **2**, (c) powder **3**, and (d) powder **4**.

(a)



(b)



(c)

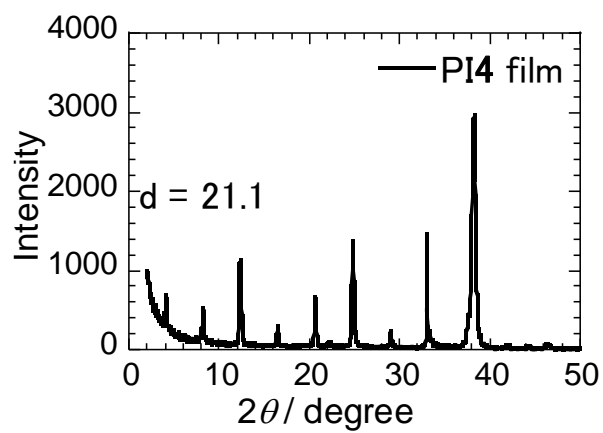
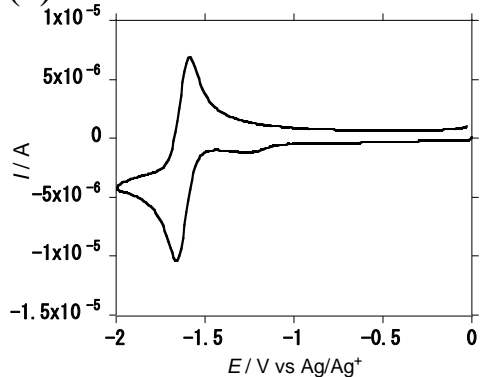


Fig. S7B XRD patterns of (a) films **2** deposited at RT and 100 °C, (b) film **3**, and (c) film **4**.

8. Redox properties

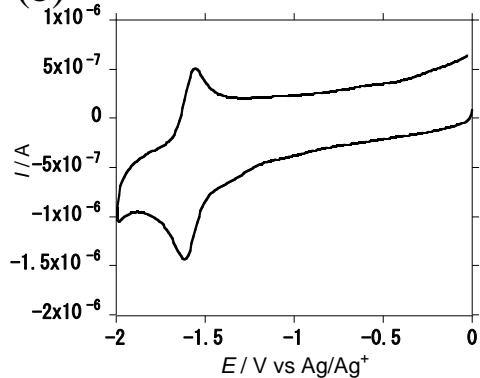
(a)



$$E_{red} = -1.62 \text{ V}$$

$$(-1.68 \text{ vs Fc/Fc}^+)$$

(b)

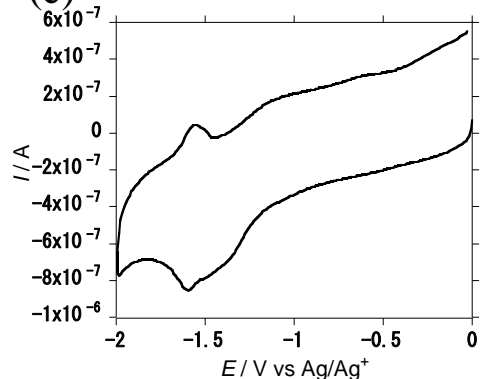


$$E_{red} = -1.58 \text{ V}$$

$$(-1.64 \text{ vs Fc/Fc}^+)$$

3.2 eV
vs Fc 4.8 eV

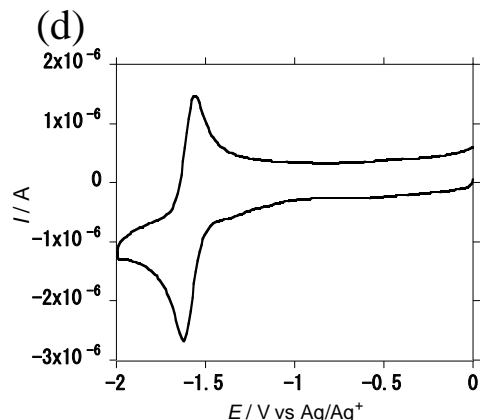
(c)



$$E_{red} = -1.57 \text{ V}$$

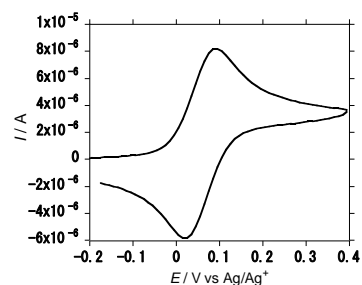
$$(-1.63 \text{ vs Fc/Fc}^+)$$

(e)



$$E_{red} = -1.59 \text{ V}$$

$$(-1.65 \text{ vs Fc/Fc}^+)$$



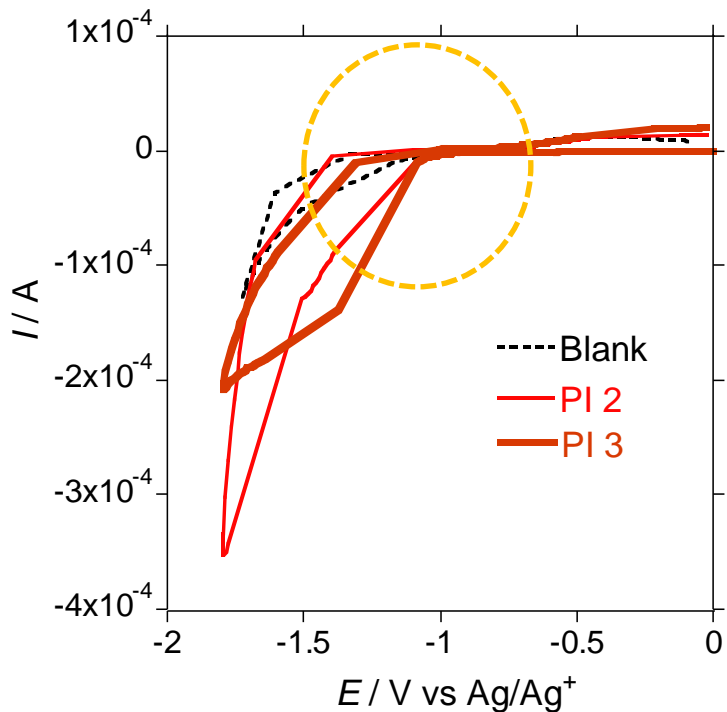
$$E_{ox} = +0.06 \text{ V}$$

$$\text{vs Ag/Ag}^+ (\text{DMF})$$

Fig. S8 Cyclic voltammograms of reduction waves of (a) PI 1, (b) 2, (c) 4, (d) 2T in DMF. (e) Oxidation wave of ferrocene in the same condition.

9. Redox properties in thin films

(a)



(b)

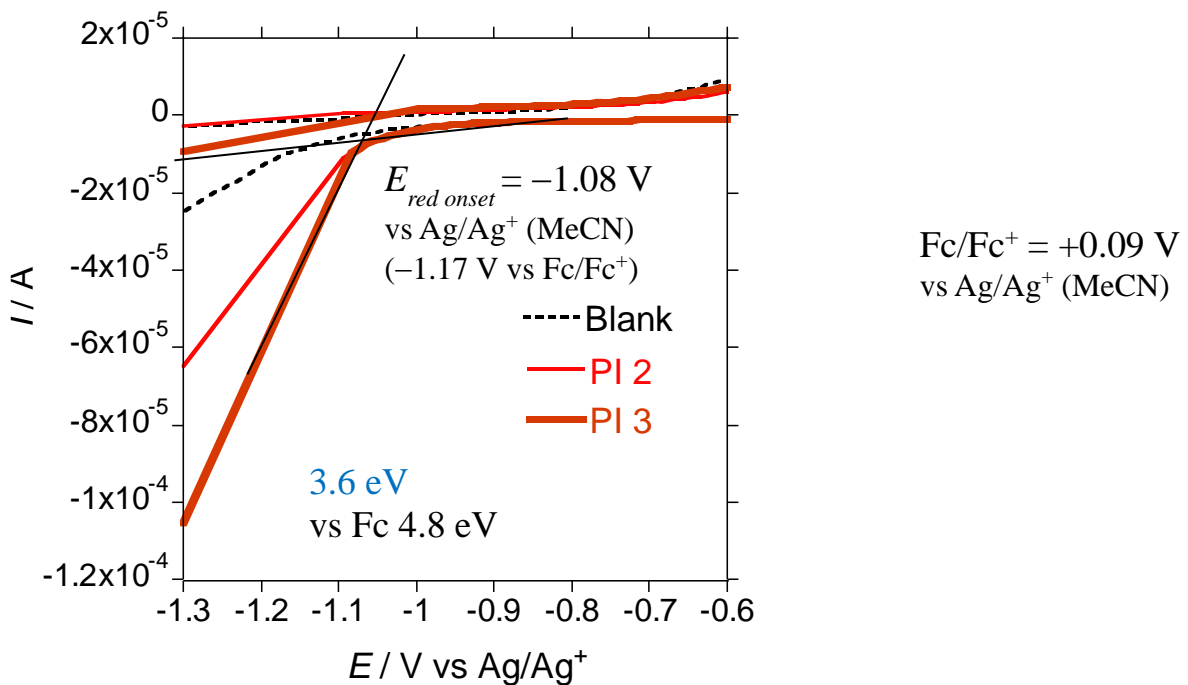


Fig. S9 (a) Cyclic voltammograms of reduction waves of thin-films of **2** and **3** deposited on ITO electrodes measured in acetonitrile (MeCN). (b) Expanded view.

10. FET measurements with LED

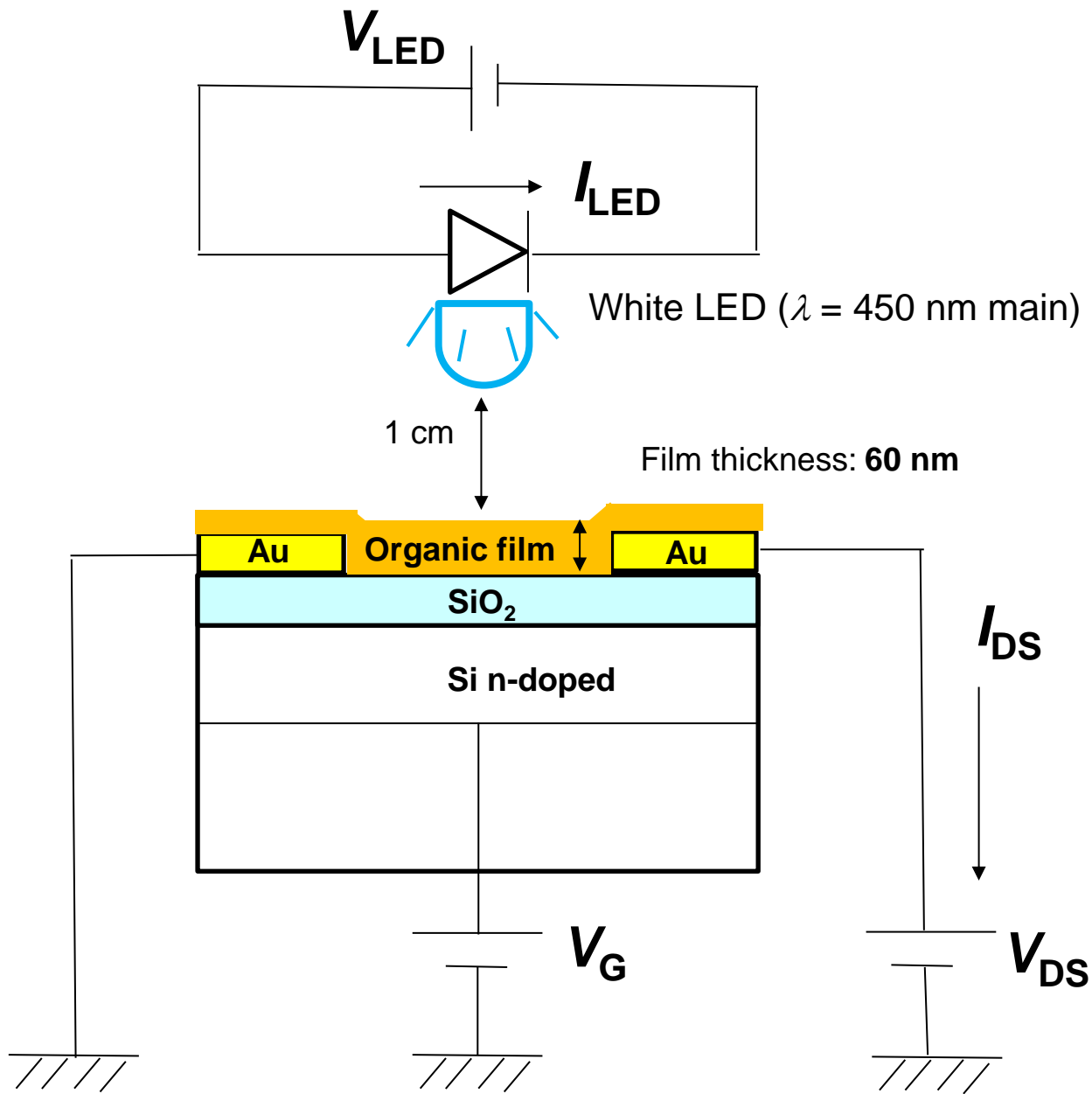
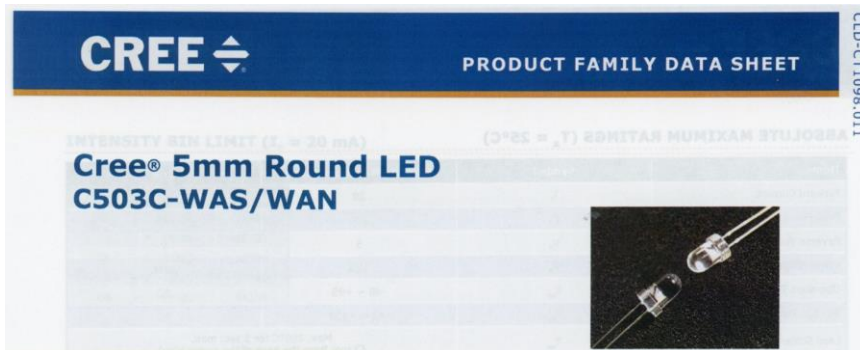


Fig. S10 An experimental image of FET and LED.

11. LED used in the measurements



C503C-WAN-CCADB231 provided by Cree Inc.

(a)

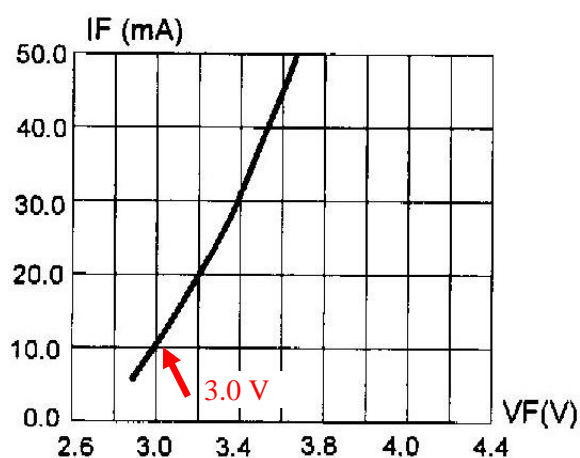


FIG.1 FORWARD CURRENT VS.
FORWARD VOLTAGE.

(b)

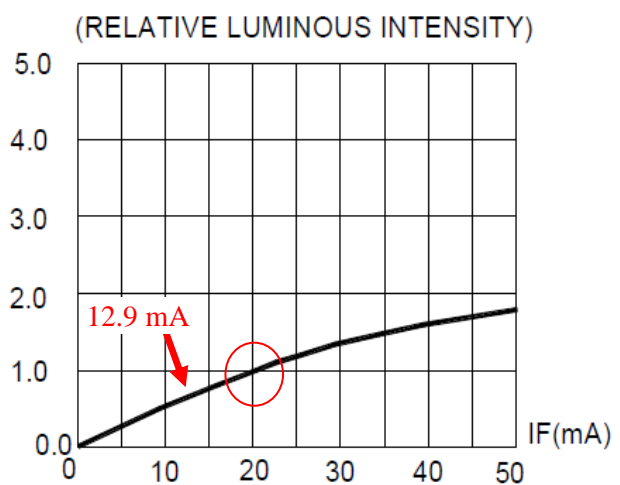


FIG.2 RELATIVE LUMINOUS INTENSITY VS.
FORWARD CURRENT

(c)

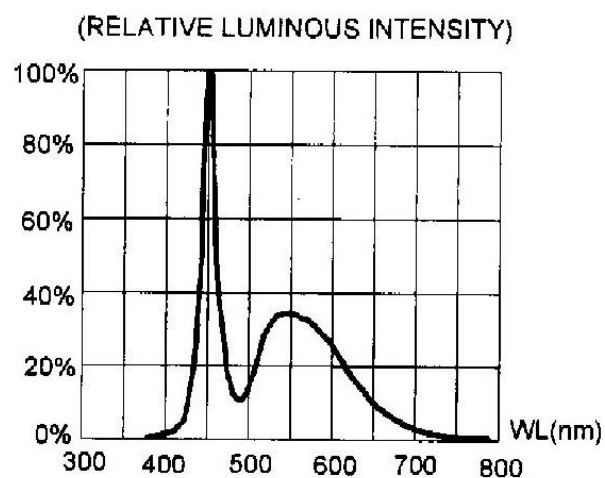


FIG.4 RELATIVE LUMINOUS INTENSITY VS.
WAVELENGTH.

Fig. S11A LED characteristics presented by Cree, Inc. (a) Forward current vs. forward voltage. (b) Relative luminous intensity vs. forward current. (c) Relative luminous intensity vs. wavelength.

Table S1 Relative luminous intensity estimated from I_{LED}

I_{LED} (mA)	0	0.01	0.28	1.00	1.75	4.86	7.72	12.9	20
Relative luminous intensity	0 ①	0.00055 ②	0.015 ③	0.055 ④	0.096 ⑤	0.27 ⑥	0.42 ⑦	0.68 ⑧	1 ^{a)}

^a Typical luminous intensity is 35000 mcd.

① ② ③ ④ ⑤ ⑥ ⑦ ⑧

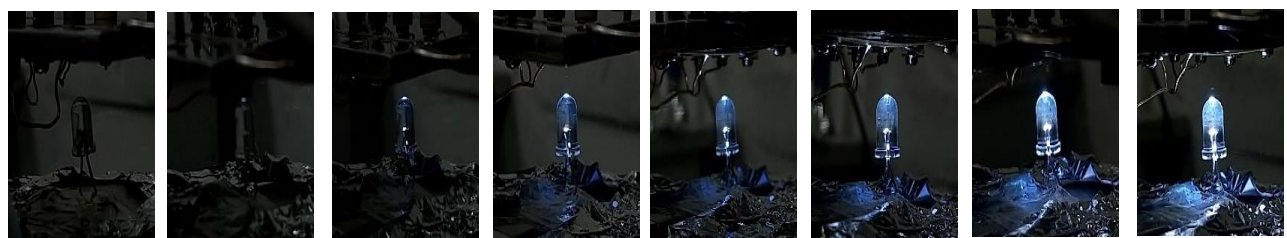
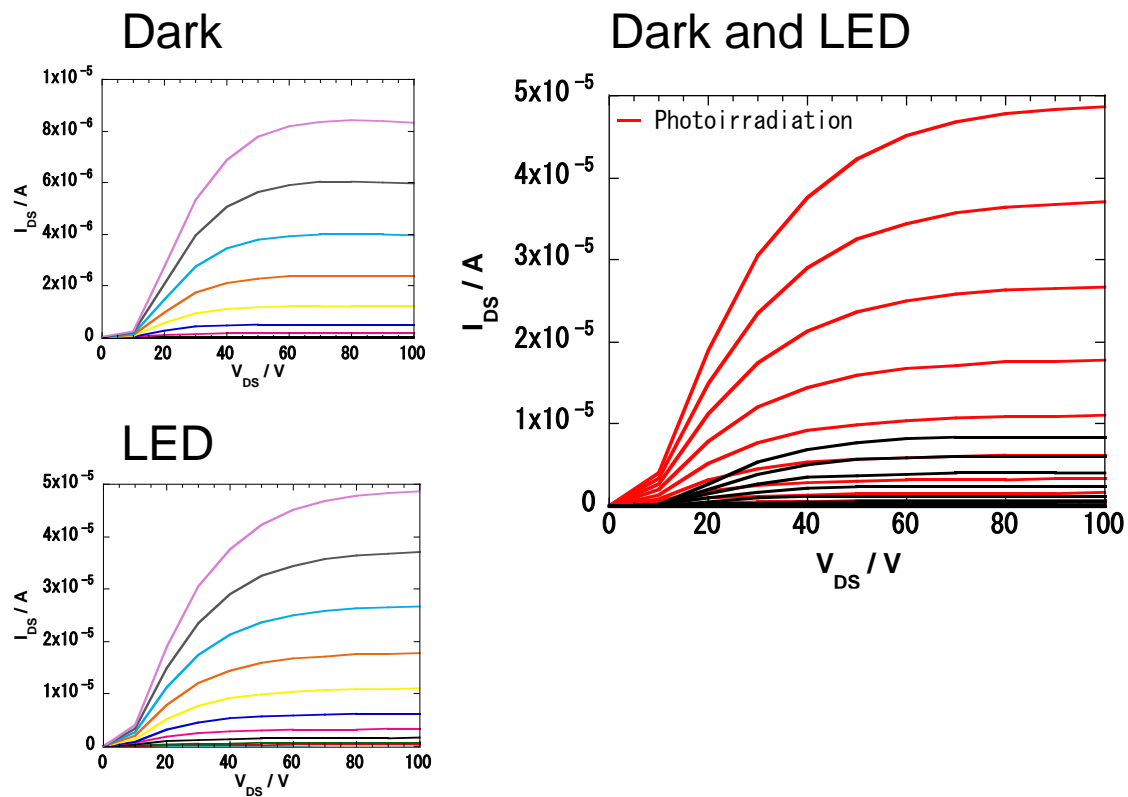
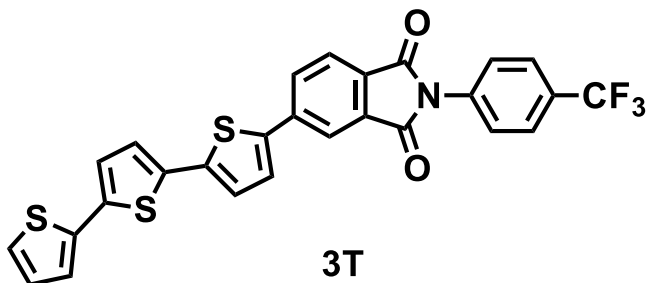


Fig. S11B Photograph images of the LED taken while changing I_{LED} .

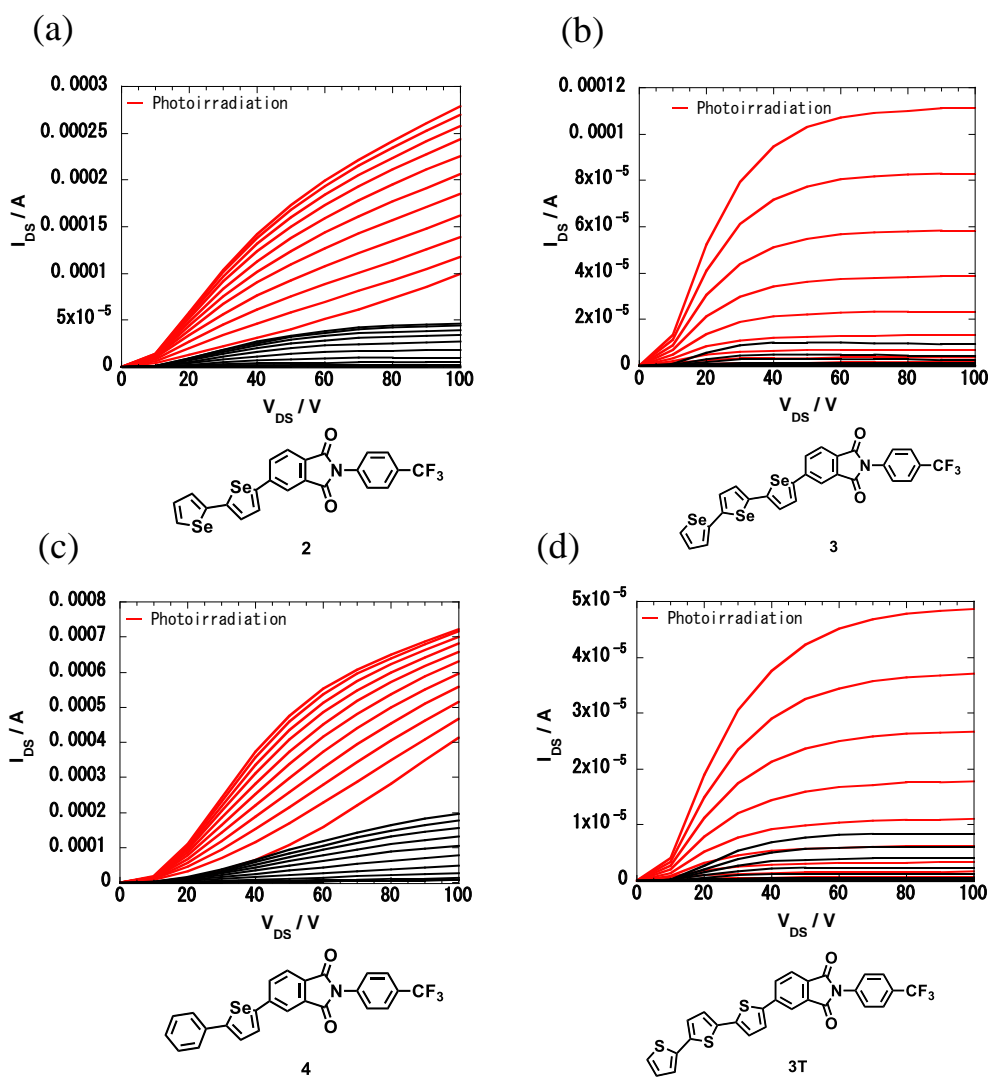
12. FET characteristics

FET of Terthiophene derivative **3T**



	Mobility (cm^2/Vs)	Threshold voltage (V)
Dark	2.9×10^{-5}	35
LED	1.2×10^{-4}	23

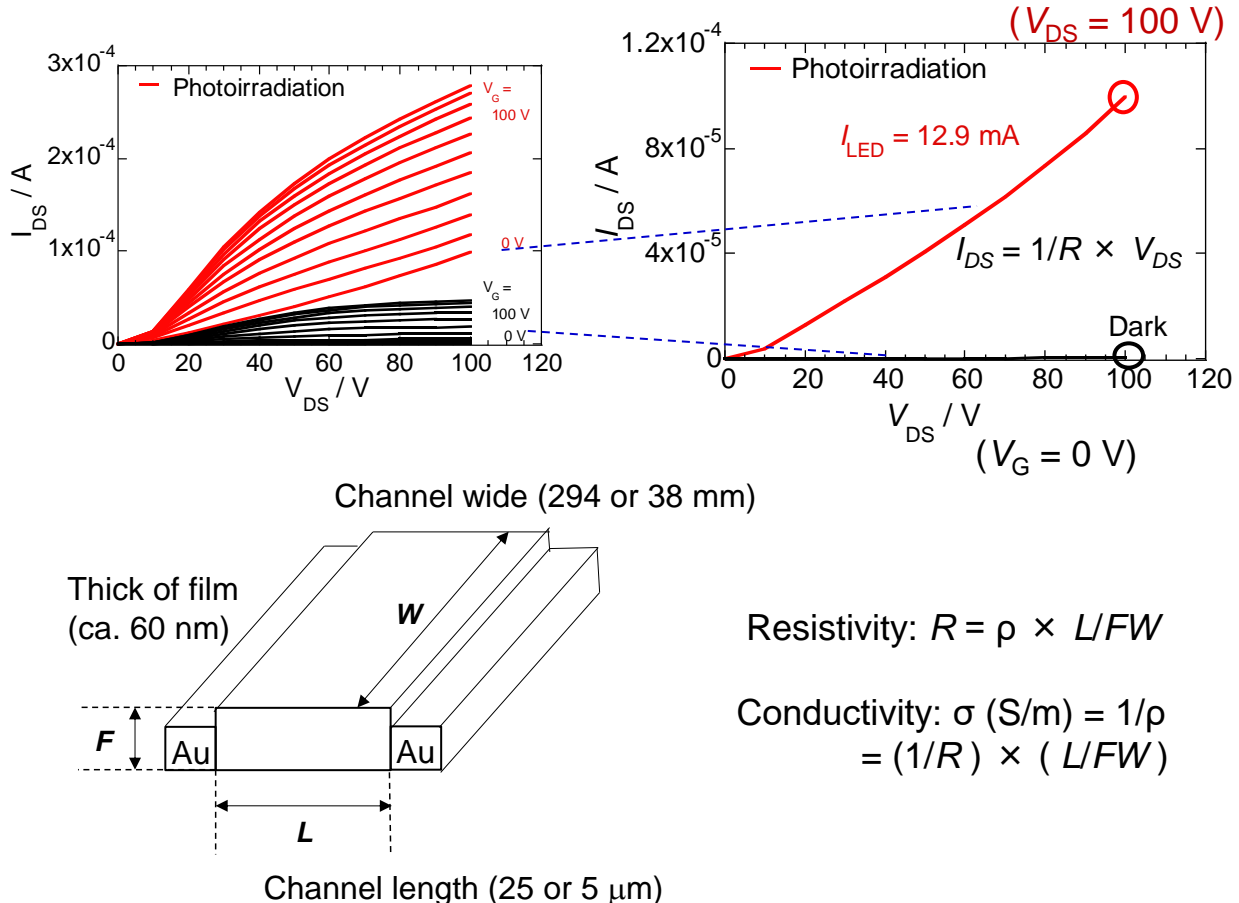
Fig. S12A FET characteristics of terthiophene derivative **3T**.



Compd	Mobility (cm^2/Vs)		Threshold voltage (V)
2	Dark	1.3×10^{-4}	5
	LED	7.7×10^{-5}	<<0
3	Dark	4.2×10^{-4}	29
	LED	1.2×10^{-3}	21
4	Dark	5.9×10^{-4}	<0
	LED	1.0×10^{-4}	<<0
3T	Dark	2.9×10^{-5}	35
	LED	1.2×10^{-4}	23

Fig. S12B FET characteristics of (a) **2** (b) **3** (c) **4**, and (d) **3T**.

13. Conductivity



2

Fig. S13 Conductivities of organic thin films in the dark and during photoirradiation.

Compound 2

Dark condition: $I_{DS} = 3.26 \times 10^{-7} \text{ A}$

$$\begin{aligned} \text{S/m} &= L/WF \times I_{DS}/V_{DS} = \{25 \times 10^{-6} \text{ m} / 294 \times 10^{-3} \text{ m} \times 60 \times 10^{-9} \text{ m}\} \times \{3.26 \times 10^{-7} / 100 \text{ V}\} \\ &= 4.62 \times 10^{-6} \end{aligned}$$

LED condition: $I_{DS} = 9.95 \times 10^{-5} \text{ A}$

$$\begin{aligned} \text{S/m} &= L/WF \times I_{DS}/V_{DS} = \{25 \times 10^{-6} \text{ m} / 294 \times 10^{-3} \text{ m} \times 60 \times 10^{-9} \text{ m}\} \times \{9.95 \times 10^{-5} / 100 \text{ V}\} \\ &= 1.41 \times 10^{-3} \end{aligned}$$

Compound 3

Dark condition: $I_{DS} = 1.40 \times 10^{-8} \text{ A}$

$$\begin{aligned} \text{S/m} &= L/WF \times I_{DS}/V_{DS} = \{25 \times 10^{-6} \text{ m} / 294 \times 10^{-3} \text{ m} \times 60 \times 10^{-9} \text{ m}\} \times \{1.40 \times 10^{-8} / 100 \text{ V}\} \\ &= 1.98 \times 10^{-7} \end{aligned}$$

LED condition: $I_{DS} = 2.70 \times 10^{-6} \text{ A}$

$$\text{S/m} = L/WF \times I_{DS}/V_{DS} = \{25 \times 10^{-6} \text{ m} / 294 \times 10^{-3} \text{ m} \times 60 \times 10^{-9} \text{ m}\} \times \{2.70 \times 10^{-6} / 100 \text{ V}\}$$

$$= 3.82 \times 10^{-5}$$

Compound 4

Dark condition: $I_{DS} = 7.57 \times 10^{-6} \text{ A}$

$$\begin{aligned} S/m &= L/WF \times I_{DS} / V_{DS} = \{5 \times 10^{-6} \text{ m} / 38 \times 10^{-3} \text{ m} \times 60 \times 10^{-9} \text{ m}\} \times \{7.57 \times 10^{-6} / 100 \text{ V}\} \\ &= 1.66 \times 10^{-4} \end{aligned}$$

LED condition: $I_{DS} = 3.46 \times 10^{-4} \text{ A}$

$$\begin{aligned} S/m &= L/WF \times I_{DS} / V_{DS} = \{5 \times 10^{-6} \text{ m} / 38 \times 10^{-3} \text{ m} \times 60 \times 10^{-9} \text{ m}\} \times \{3.46 \times 10^{-4} / 100 \text{ V}\} \\ &= 7.59 \times 10^{-3} \end{aligned}$$

Compound 3T

Dark condition: $I_{DS} = 5.44 \times 10^{-9} \text{ A}$

$$\begin{aligned} S/m &= L/WF \times I_{DS} / V_{DS} = \{25 \times 10^{-6} \text{ m} / 294 \times 10^{-3} \text{ m} \times 60 \times 10^{-9} \text{ m}\} \times \{5.44 \times 10^{-9} / 100 \text{ V}\} \\ &= 7.71 \times 10^{-8} \end{aligned}$$

LED condition: $I_{DS} = 2.22 \times 10^{-7} \text{ A}$

$$\begin{aligned} S/m &= L/WF \times I_{DS} / V_{DS} = \{25 \times 10^{-6} \text{ m} / 294 \times 10^{-3} \text{ m} \times 60 \times 10^{-9} \text{ m}\} \times \{2.22 \times 10^{-7} / 100 \text{ V}\} \\ &= 3.14 \times 10^{-6} \end{aligned}$$

Table S2 Conductivities calculated from thin film of 2-4 and 3T

compounds		Conductivity at $V_G = 0 \text{ V}$ (S/m)
2	dark	4.6×10^{-6}
	LED	1.4×10^{-3}
3	dark	2.0×10^{-7}
	LED	3.8×10^{-5}
4	dark	1.7×10^{-4}
	LED	7.6×10^{-3}
3T	dark	7.7×10^{-8}
	LED	3.1×10^{-6}

14. FET made by raising substrate temperature to 100 °C during deposition

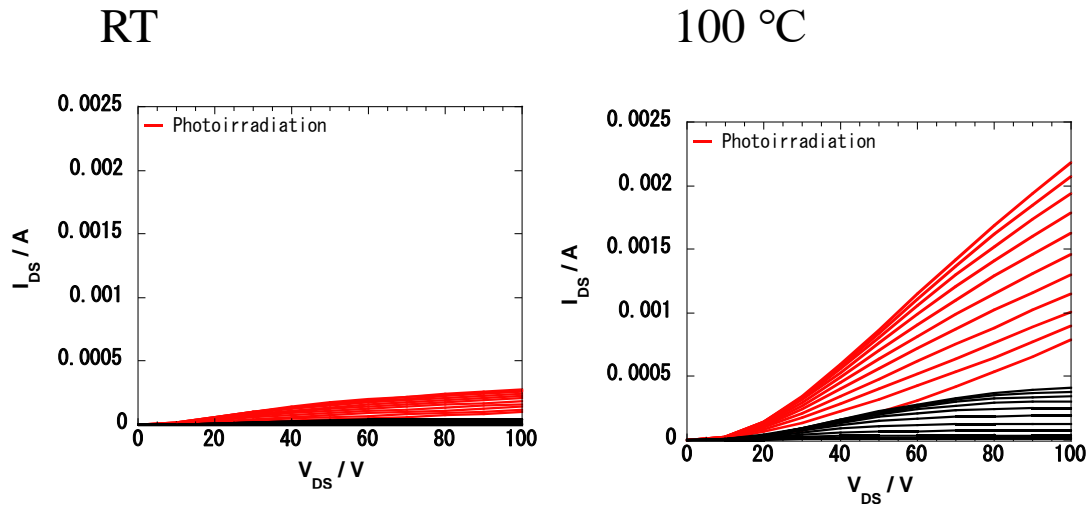


Fig. S14 FET characteristics of thin films **2** deposited at substrate temperature of RT and 100 °C.

Table S3 FET characteristics of **2** deposited at substrate temperature of RT and 100 °C

Compd		Mobility (cm ² /Vs)	Threshold voltage (V)	Conductivity at V _G = 0 V (S/m)
2 _RT	dark	1.3×10 ⁻⁴	5	4.6×10 ⁻⁶
	LED	7.7×10 ⁻⁵	<<0	1.4×10 ⁻³
2 _100°C	dark	8.9×10 ⁻⁴	<0	1.1×10 ⁻⁴
	LED	6.6×10 ⁻⁴	<<0	9.7×10 ⁻³

15. Changes of FET output characteristics depending on I_{LED}

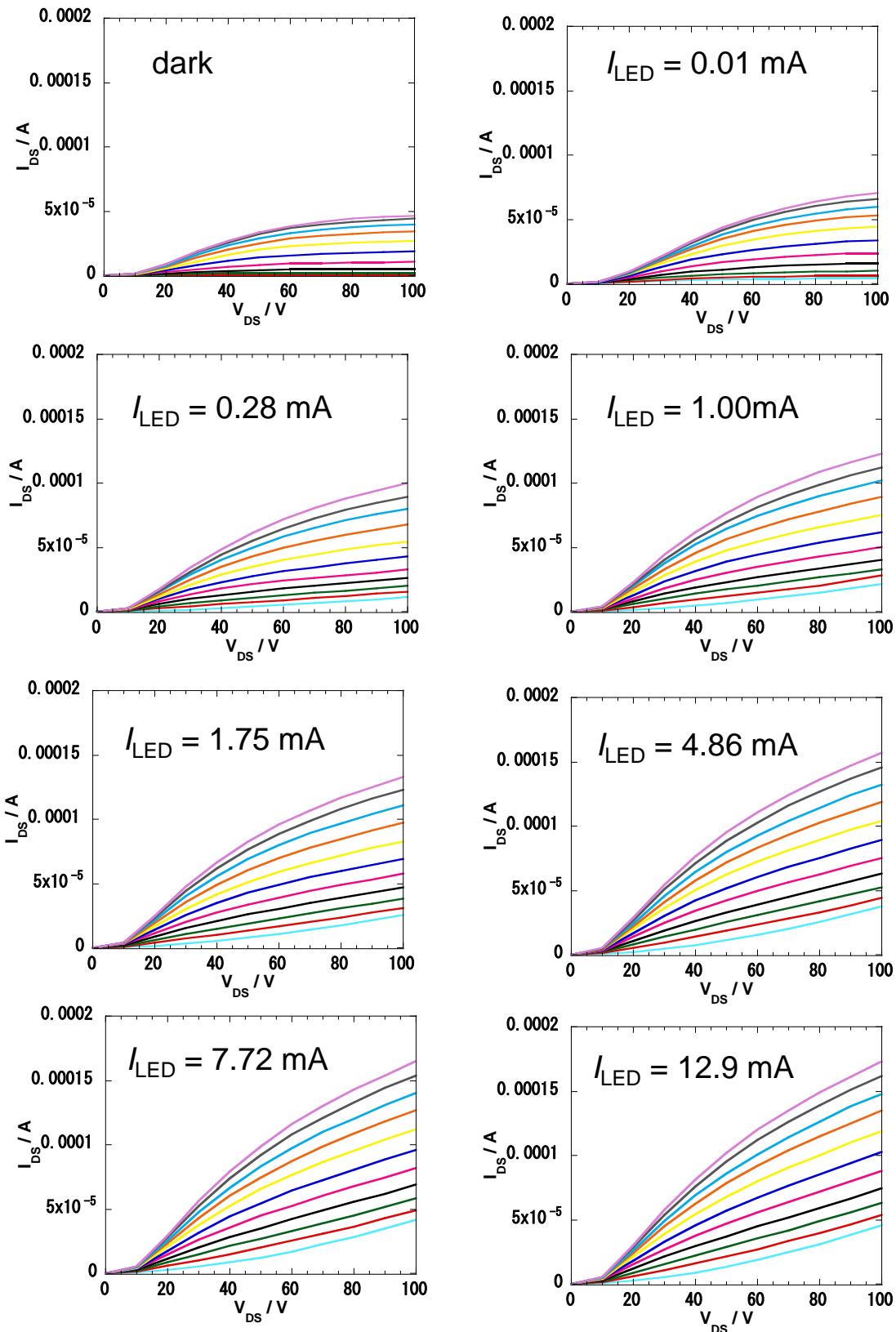


Fig. S15 FET output characteristics of **2** depending on I_{LED} . (depositited at RT)

16. Changes of FET transfer characteristics depending on I_{LED}

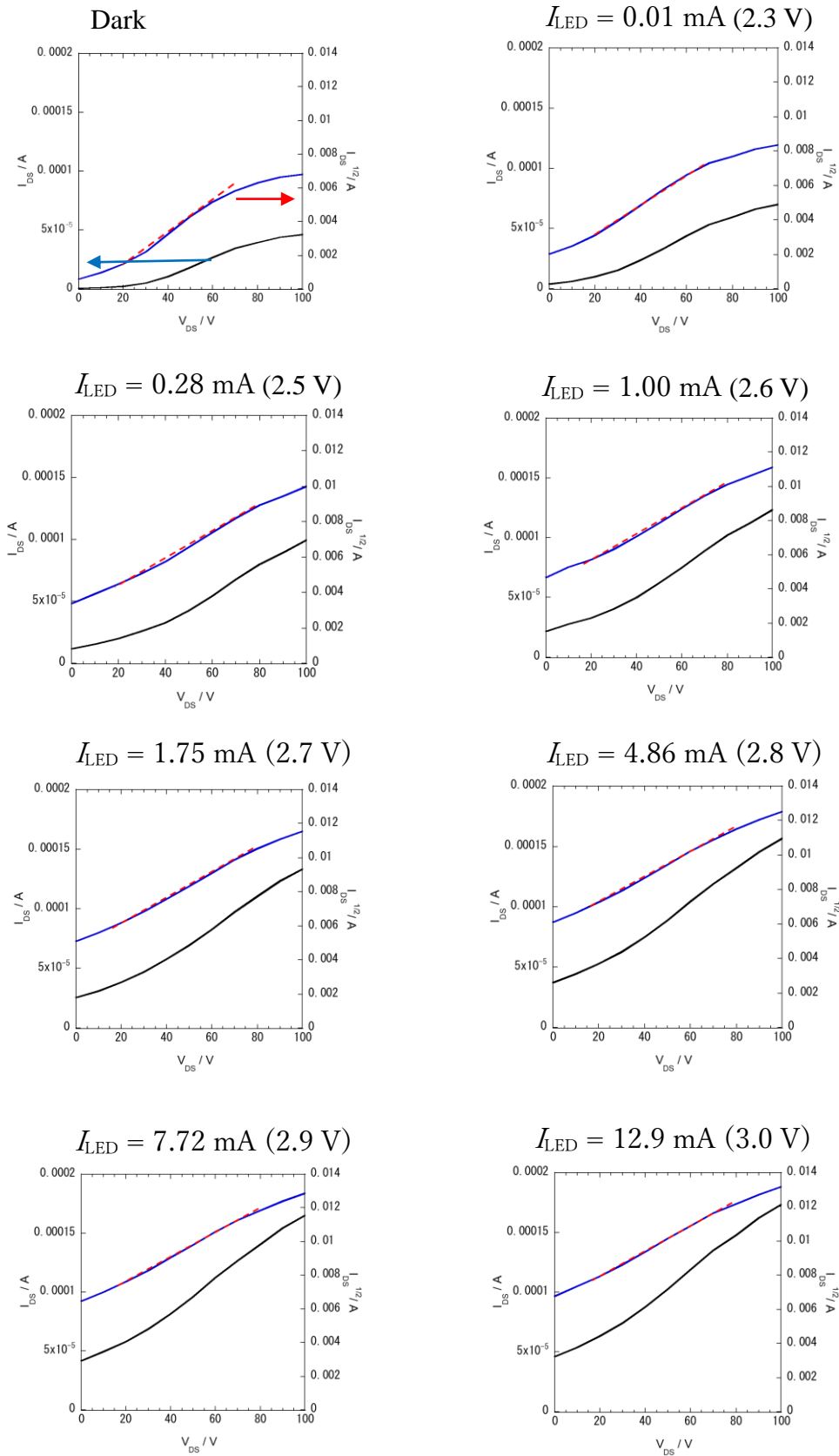


Fig. S16 FET transfer characteristics of **2** depending on I_{LED} . (depositited at RT)

17. Molecular orbitals and TD-DFT calculations

Calculations were carried out using Chem3D Pro 7.0 and Gaussian 09. The structures of imides were first optimized by the MM2 level of theory implemented in Chem3D. From the structures, the molecular geometries were again optimized by the semi-empirical calculation using RPM3 method implemented in Gaussian 09. From the structures, the ground state geometries were finally optimized in the gas phase by DFT using the RB3LYP functional and 6-31G(d,p) basis set with Gaussian 09. With the geometries, TD-DFT calculations were carried by using the B3LYP 6-31G(d,p) to estimate some S_n states, and oscillator strengths f in the transitions.

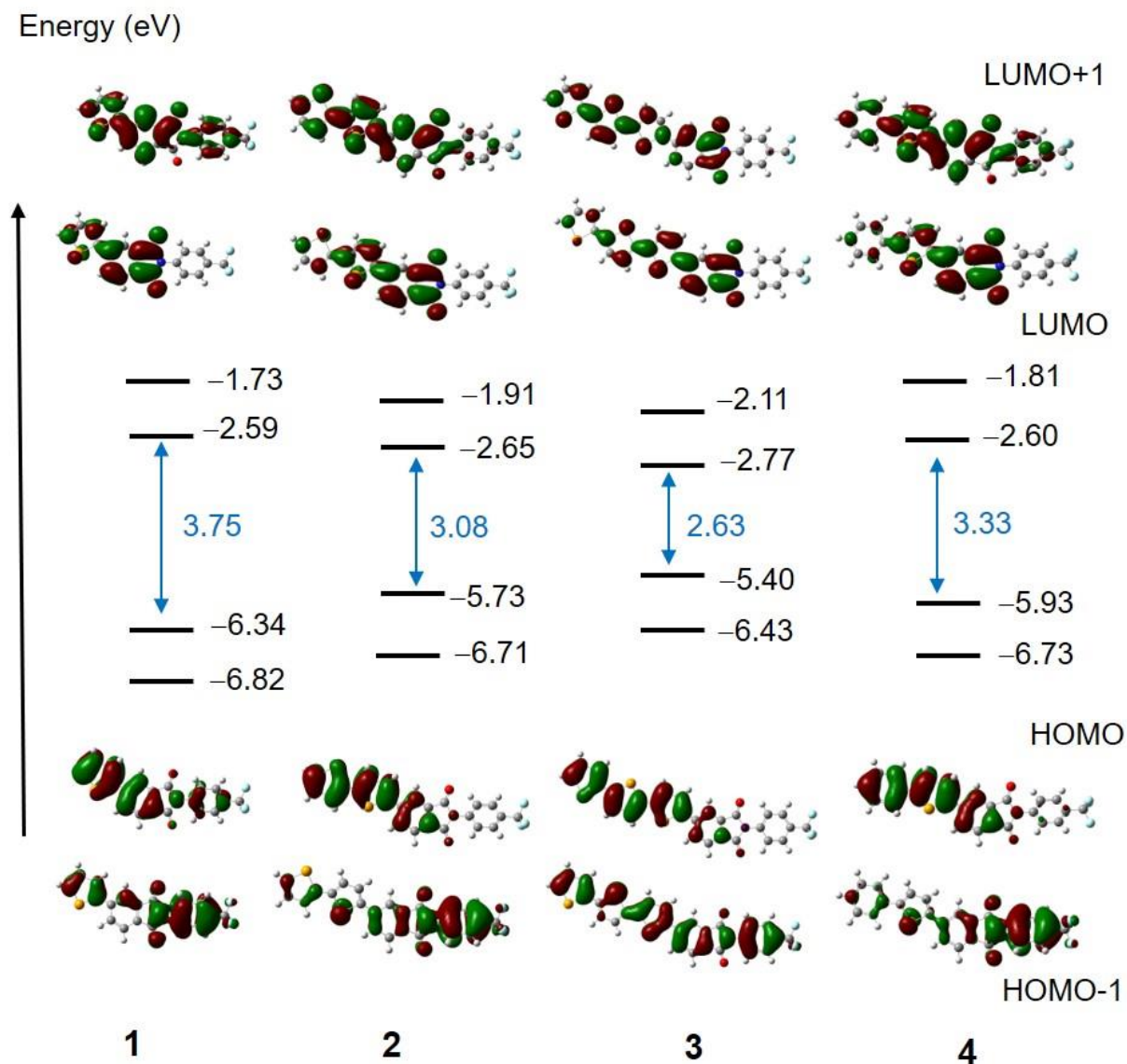


Figure S17 Molecular orbitals of **1–4** performed using Gaussian 09 at RB3LYP/6-31G(d,p) levels of theory.

PI 1

Calculation Type = FOPT

Calculation Method = RB3LYP

Basis Set = 6-31G(D,P)

Charge = 0

Spin = Singlet

Electronic Energy = -3634.1956 Hartree

RMS Gradient Norm = 5.2585774e-06 Hartree/Bohr

Dipole Moment = 6.608 Debye

Tag	Symbol	X	Y	Z
1	C	-0.89397	-0.16972	-0.06804
2	C	-0.7288	1.193681	-0.30391
3	C	0.721688	1.503817	-0.32091
4	N	1.386301	0.264193	-0.08558
5	C	0.451161	-0.79267	0.076939
6	C	-2.14283	-0.7557	0.016825
7	C	-3.28124	0.064069	-0.15868
8	C	-3.09536	1.444284	-0.40301
9	C	-1.82814	2.024263	-0.47293
10	C	2.799972	0.107665	-0.02366
11	C	3.591221	1.110789	0.551778
12	C	4.972636	0.955743	0.604385
13	C	5.572486	-0.20024	0.100691
14	C	4.781012	-1.20195	-0.46469
15	C	3.399825	-1.05089	-0.53461
16	C	-4.6212	-0.5206	-0.09481
17	O	0.717401	-1.95673	0.288001
18	O	1.26136	2.575696	-0.49491
19	C	-4.97964	-1.82802	-0.32123
20	C	-6.36843	-2.12357	-0.19766
21	C	-7.15428	-1.05765	0.133498
22	Se	-6.15076	0.499186	0.332402
23	C	7.069499	-0.33938	0.113456
24	F	7.630373	0.170979	-1.00885
25	F	7.454685	-1.63315	0.18815
26	F	7.627135	0.312311	1.158665
27	H	-2.23823	-1.81332	0.235341
28	H	-3.96985	2.069287	-0.55878
29	H	-1.70318	3.08536	-0.66107
30	H	3.12959	2.007464	0.941957
31	H	5.584481	1.730672	1.052489

32	H	5.243854	-2.10372	-0.84972
33	H	2.788759	-1.83251	-0.96486
34	H	-4.25341	-2.58188	-0.60589
35	H	-6.76879	-3.11851	-0.36026
36	H	-8.2248	-1.05093	0.281224

Table S4 The selected absorption peaks of **1** calculated by TD-DFT method^a

	Excited state	Energy (eV)	Wavelength (nm)	Oscillator strength: <i>f</i>	Main transition configuration (CI coefficient)
1	S1	3.25	381	0.1520	HOMO → LUMO (0.664)
	S2	3.68	337	0.0808	HOMO-1→ LUMO (0.642)
	S6	4.07	304	0.4226	HOMO→ LUMO+1 (0.619)

^aCalculated at the B3LYP/6-31G(d,p) level of theory.

PI 2

Calculation Type = FOPT

Calculation Method = RB3LYP

Basis Set = 6-31G(d,p)

Charge = 0

Spin = Singlet

E(RB3LYP) = -6187.20348385 a.u.

RMS Gradient Norm = 0.00000299 a.u.

Dipole Moment = 7.5641 Debye

Row	Symbol	X	Y	Z
1	C	-1.02396	0.583554	-0.15919
2	C	-0.71322	1.963734	-0.12352
3	C	0.600119	2.431352	-0.08173
4	C	1.62107	1.490427	-0.08586
5	C	1.333327	0.127024	-0.12252
6	C	0.038107	-0.35184	-0.15374
7	C	3.092056	1.668119	-0.04983
8	N	3.642756	0.351624	-0.06256
9	C	2.616459	-0.62922	-0.10323
10	C	-2.40734	0.120588	-0.20562
11	O	2.775787	-1.83138	-0.12003
12	O	3.726588	2.701074	-0.01521
13	C	5.036259	0.062197	-0.03385
14	C	5.938298	0.893867	-0.71062
15	C	7.3003	0.612719	-0.67181

16	C	7.770798	-0.50228	0.024087
17	C	6.868798	-1.33544	0.689301
18	C	5.506472	-1.05541	0.669028
19	C	9.247038	-0.77314	0.110692
20	F	9.511975	-2.09668	0.192491
21	F	9.798343	-0.19728	1.20583
22	F	9.913506	-0.2902	-0.96178
23	C	-2.87462	-1.1051	-0.62309
24	C	-4.27954	-1.28308	-0.58745
25	C	-5.01357	-0.20787	-0.13665
26	Se	-3.85661	1.208434	0.326855
27	C	-6.44348	-0.09013	-0.00157
28	Se	-7.57548	-1.60353	-0.04405
29	C	-9.01476	-0.43641	0.172229
30	C	-8.6018	0.861505	0.263747
31	C	-7.19346	1.0511	0.16792
32	H	-1.52581	2.684002	-0.15001
33	H	0.819427	3.493538	-0.05623
34	H	-0.14896	-1.41964	-0.15004
35	H	5.577442	1.759181	-1.2494
36	H	7.997793	1.255806	-1.19661
37	H	7.2309	-2.2067	1.223856
38	H	4.810025	-1.70724	1.17837
39	H	-2.21076	-1.87855	-0.99398
40	H	-4.75627	-2.19987	-0.91996
41	H	-10.0284	-0.80875	0.212818
42	H	-9.2928	1.687751	0.392199
43	H	-6.73463	2.03452	0.204186

Table S5 The selected absorption peaks of **2** calculated by TD-DFT method^a

	Excited state	Energy (eV)	Wavelength (nm)	Oscillator strength: <i>f</i>	Main transition configuration (CI coefficient)
2	S1	2.78	446	0.5639	HOMO → LUMO (0.696)
	S2	3.41	364	0.4420	HOMO → LUMO+1 (0.679)
	S3	3.47	357	0.0479	HOMO-1 → LUMO (0.681)

^aCalculated at the B3LYP/6-31G(d,p) level of theory.

Calculation Type = FOPT
 Calculation Method = RB3LYP
 Basis Set = 6-31G(d,p)
 Charge = 0
 Spin = Singlet
 E(RB3LYP) = -8740.20925406 a.u.
 RMS Gradient Norm = 0.00001775 a.u.
 Dipole Moment = 8.8249 Debye

Row	Symbol	X	Y	Z
1	C	3.502873	0.152737	-0.00079
2	C	3.813317	1.50702	-0.00075
3	C	5.282787	1.660263	-0.00049
4	N	5.832096	0.332693	-0.00036
5	C	4.770503	-0.62255	-0.00056
6	C	2.202121	-0.30953	-0.00095
7	C	1.151168	0.639825	-0.00114
8	C	1.488184	2.015835	-0.00111
9	C	2.807702	2.46467	-0.00089
10	C	7.229156	0.015445	-8.5E-05
11	C	8.19495	1.040496	-0.00102
12	C	9.547576	0.723604	-0.00075
13	C	9.972654	-0.60638	0.000434
14	C	9.019606	-1.62161	0.001355
15	C	7.659273	-1.32272	0.001115
16	C	-0.23965	0.202075	-0.00134
17	O	4.87082	-1.83231	-0.00053
18	O	5.902857	2.703809	-0.00032
19	C	-0.72398	-1.08845	-0.00313
20	C	-2.13046	-1.23144	-0.003
21	C	-2.85944	-0.0596	-0.00108
22	Se	-1.68614	1.419216	0.000933
23	C	-4.28547	0.104543	-0.00054
24	Se	-5.46064	-1.37862	-0.00057
25	C	-6.9026	-0.15631	0.000196
26	C	-6.42043	1.135199	0.000461
27	C	-5.01325	1.275429	6.45E-05
28	C	-8.27147	-0.6015	0.000439
29	C	-8.75154	-1.89181	-7.6E-06
30	C	-10.1688	-2.03027	0.000401

31	C	-10.8618	-0.85447	0.001184
32	Se	-9.71674	0.619157	0.001503
33	C	11.44441	-0.90606	0.00075
34	F	12.06047	-0.3775	-1.08373
35	F	11.70094	-2.23203	0.001499
36	F	12.06024	-0.37633	1.084793
37	H	2.009997	-1.37588	-0.0008
38	H	0.692213	2.754691	-0.0014
39	H	3.043173	3.523588	-0.00088
40	H	7.887179	2.073802	-0.00192
41	H	10.27817	1.526216	-0.00148
42	H	9.334454	-2.65878	0.00228
43	H	6.937878	-2.12402	0.001819
44	H	-0.06988	-1.95316	-0.00475
45	H	-2.61151	-2.20458	-0.00447
46	H	-7.08569	1.99306	0.000893
47	H	-4.53117	2.248383	0.000111
48	H	-8.08579	-2.74973	-0.00065
49	H	-10.6585	-2.99818	0.000105
50	H	-11.9342	-0.72179	0.001601

Table S6 The selected absorption peaks of **3** calculated by TD-DFT method^a

	Excited state	Energy (eV)	Wavelength (nm)	Oscillator strength: <i>f</i>	Main transition configuration (CI coefficient)
3	S1	2.40	517	0.9982	HOMO → LUMO (0.703)
	S2	2.97	417	0.5157	HOMO → LUMO+1 (0.688)
	S3	3.17	391	0.0037	HOMO-1 → LUMO (0.649)

^aCalculated at the B3LYP/6-31G(d,p) level of theory.

PI 4

Calculation Type = FOPT

Calculation Method = RB3LYP

Basis Set = 6-31G(D,P)

Charge = 0

Spin = Singlet

Solvation = None

Electronic Energy = -3865.2647 Hartree

RMS Gradient Norm = 5.274755e-06 Hartree/Bohr

Dipole Moment = 7.4683395 Debye

Row	Symbol	X	Y	Z
1	C	0.747726	0.015344	-0.12476
2	C	0.974193	1.388698	-0.05023
3	C	2.435947	1.629817	0.00969
4	N	3.043794	0.339781	-0.02647
5	C	2.062525	-0.68407	-0.10487
6	C	-0.52499	-0.51879	-0.18571
7	C	-1.62625	0.369171	-0.18256
8	C	-1.37822	1.759972	-0.10797
9	C	-0.08717	2.283658	-0.03621
10	O	2.276168	-1.87706	-0.1473
11	O	3.024083	2.688303	0.076921
12	C	4.447827	0.1089	0.012543
13	C	5.32142	0.989725	-0.63921
14	C	6.692956	0.762762	-0.59223
15	C	7.20225	-0.34403	0.090257
16	C	6.329421	-1.22288	0.734449
17	C	4.956873	-0.99748	0.705252
18	C	-2.98783	-0.15387	-0.26114
19	C	-3.3953	-1.36888	-0.76192
20	C	-4.79197	-1.61793	-0.73392
21	C	-5.57286	-0.6156	-0.20819
22	Se	-4.4854	0.819654	0.345068
23	C	-7.02892	-0.58906	-0.05325
24	C	-7.75053	-1.78913	0.091808
25	C	-9.13661	-1.77514	0.220109
26	C	-9.8337	-0.56503	0.217477
27	C	-9.13045	0.633177	0.08176
28	C	-7.74505	0.622025	-0.05688
29	C	8.680415	-0.61829	0.079541
30	F	9.047294	-1.34874	-1.00065
31	F	9.073181	-1.31184	1.17151
32	F	9.403801	0.523498	0.040687
33	H	-0.6671	-1.59333	-0.20991
34	H	-2.22288	2.442523	-0.12777
35	H	0.084866	3.353416	0.018693
36	H	4.930655	1.852735	-1.1607

37	H	7.369396	1.450886	-1.08695
38	H	6.723141	-2.07778	1.272649
39	H	4.283332	-1.68051	1.204593
40	H	-2.69559	-2.07853	-1.19073
41	H	-5.2234	-2.52721	-1.13834
42	H	-7.21581	-2.73291	0.12878
43	H	-9.67334	-2.71228	0.334602
44	H	-10.9142	-0.55612	0.322852
45	H	-9.66266	1.579693	0.073467
46	H	-7.21005	1.558254	-0.19213

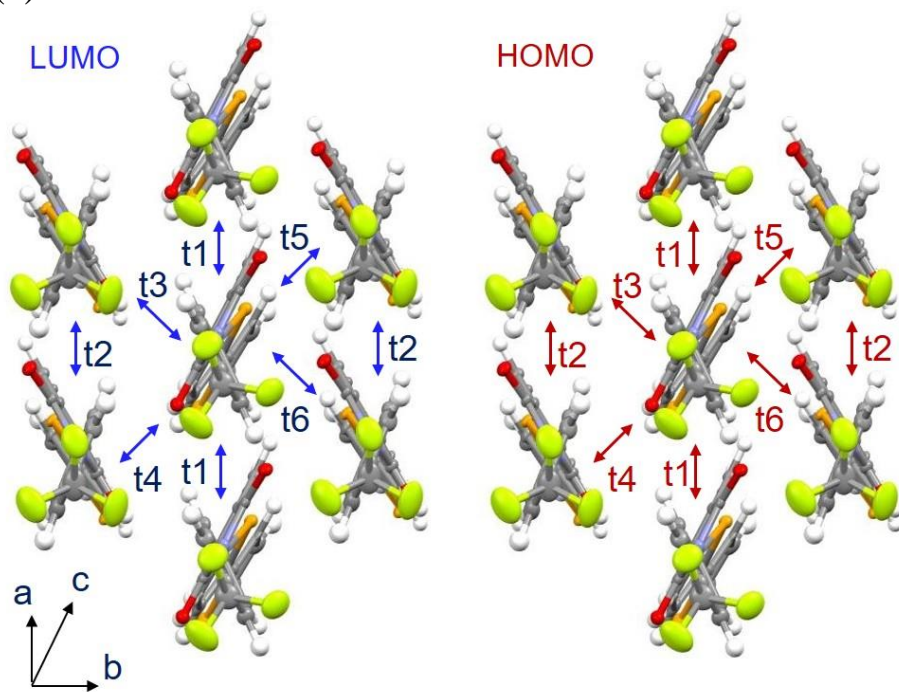
Table S7 The selected absorption peaks of **4** calculated by TD-DFT method^a

	Excited state	Energy (eV)	Wavelength (nm)	Oscillator strength: <i>f</i>	Main transition configuration (CI coefficient)
4	S1	2.97	418	0.4699	HOMO → LUMO (0.691)
	S2	3.54	351	0.0223	HOMO-1 → LUMO (0.681)
	S3	3.65	340	0.5803	HOMO → LUMO+1 (0.678)

^aCalculated at the B3LYP/6-31G(d,p) level of theory.

18. Overlap integrals of biselenophene derivative 2 and bithiophene derivative 2T.

(a)



(b)

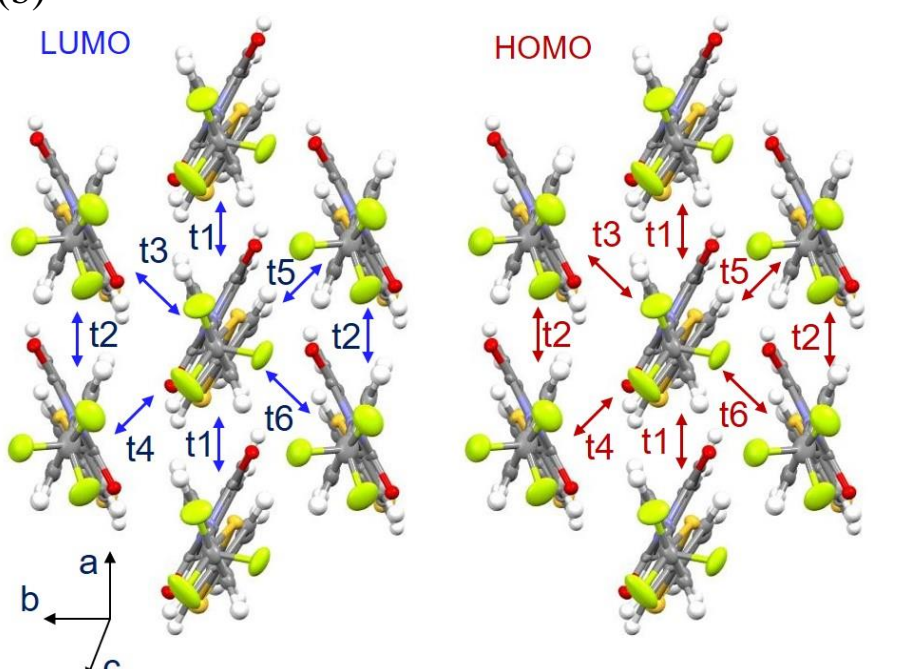


Fig. S18 (a) Overlap integrals of (a) biselenophene derivative 2 and (b) bithiophene derivative 2T.

19. $^1\text{H-NMR}$ data

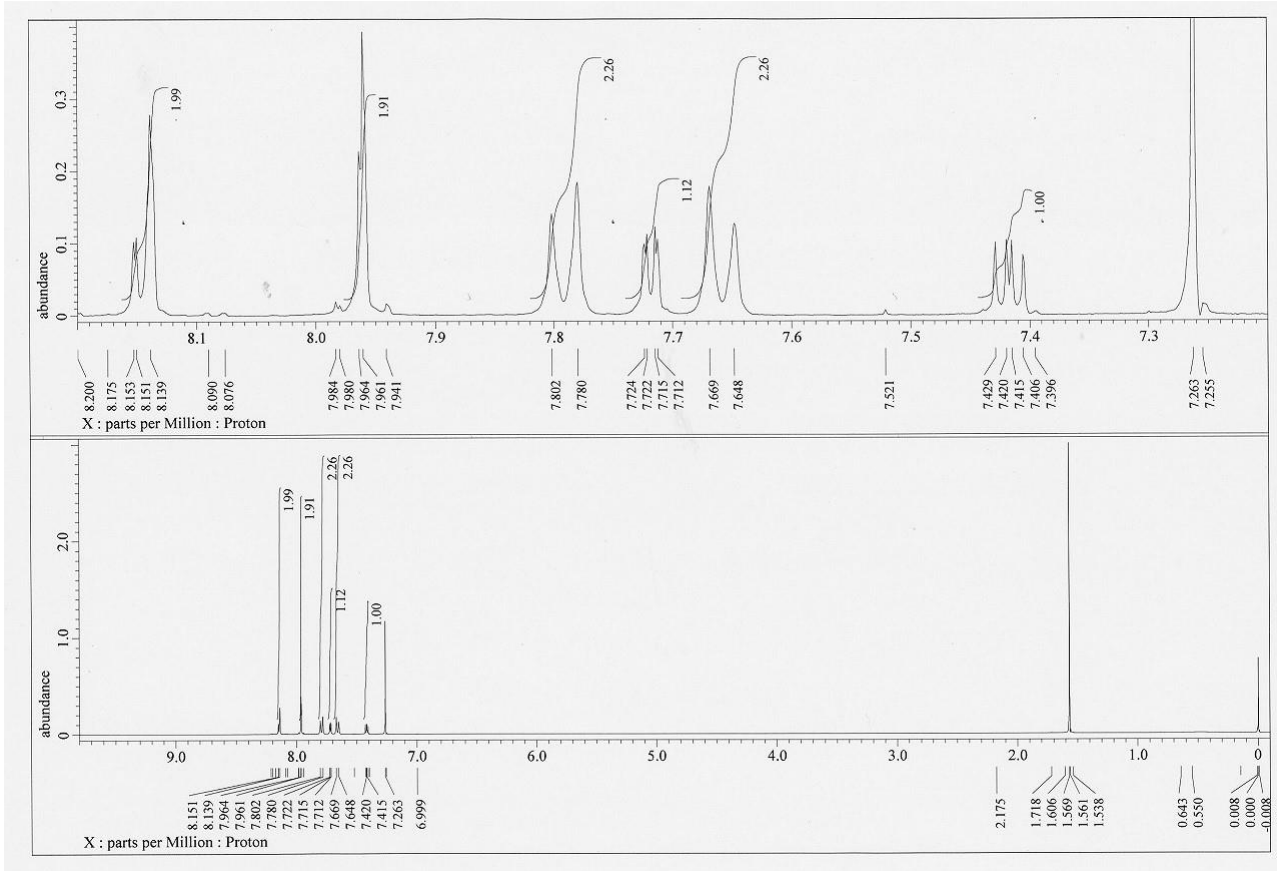


Fig. S19-1 $^1\text{H-NMR}$ spectrum of selenophene substituted PI **1** (400 MHz).

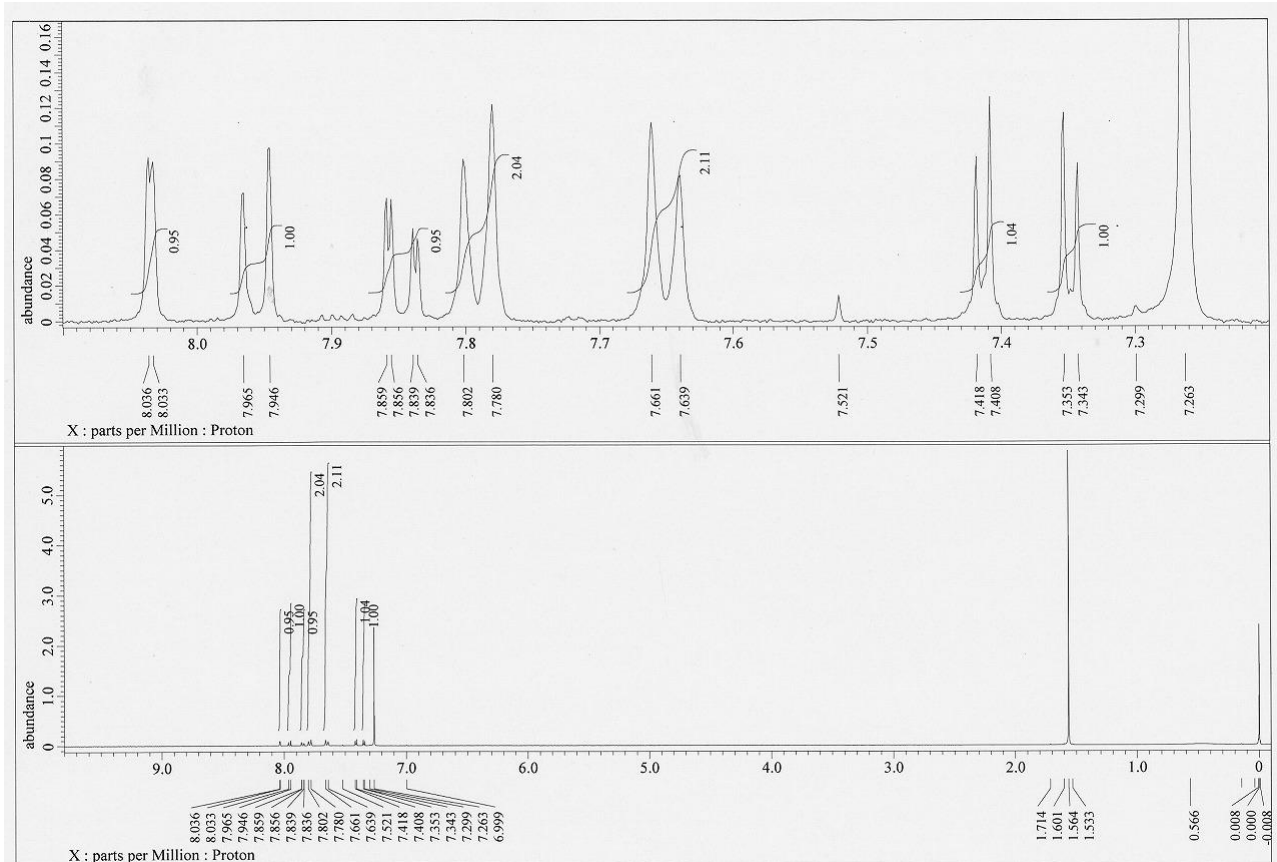


Fig. S19-2 $^1\text{H-NMR}$ spectrum of bromoselenophene substituted PI **6** (400 MHz).

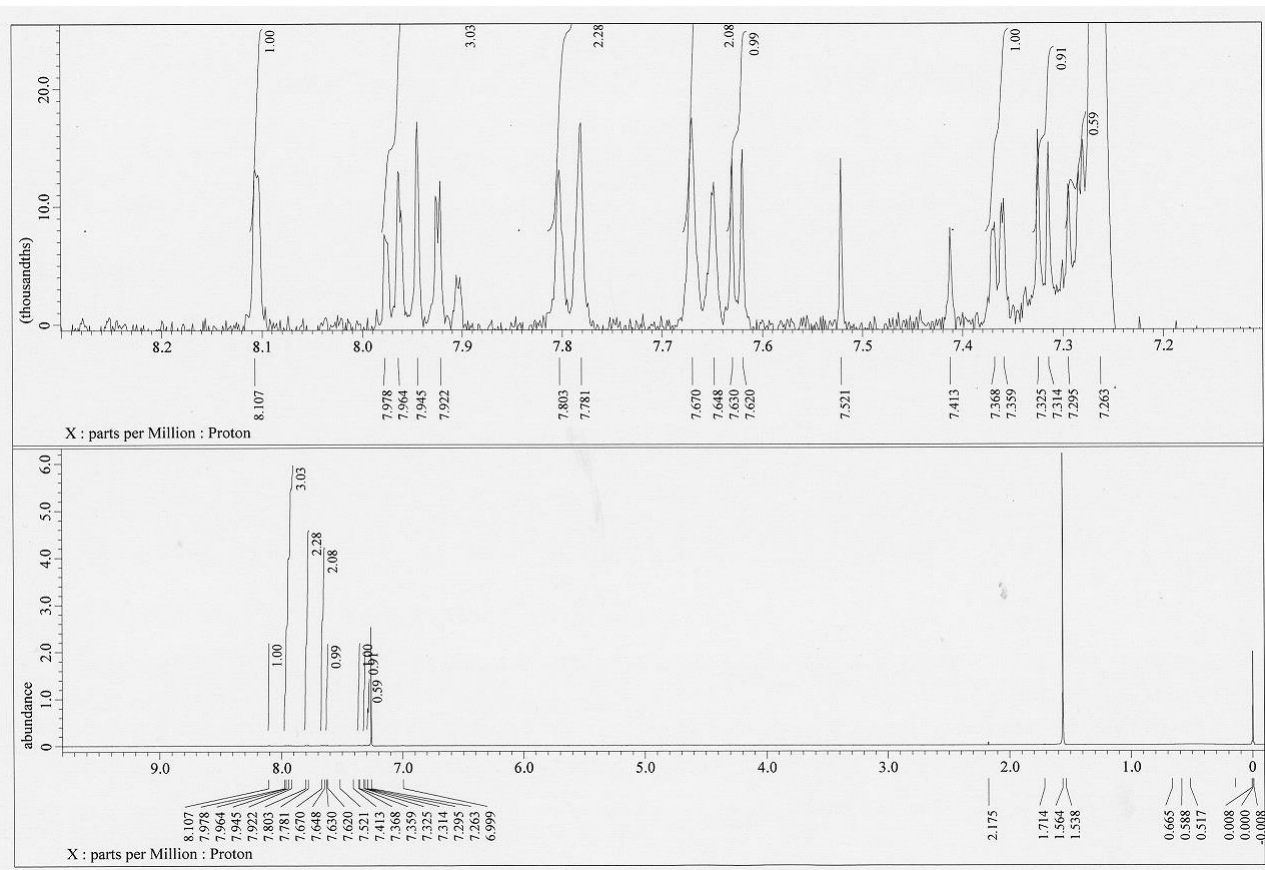


Fig. S19-3 ^1H -NMR spectrum of biselenophene substituted PI **2** (400 MHz).

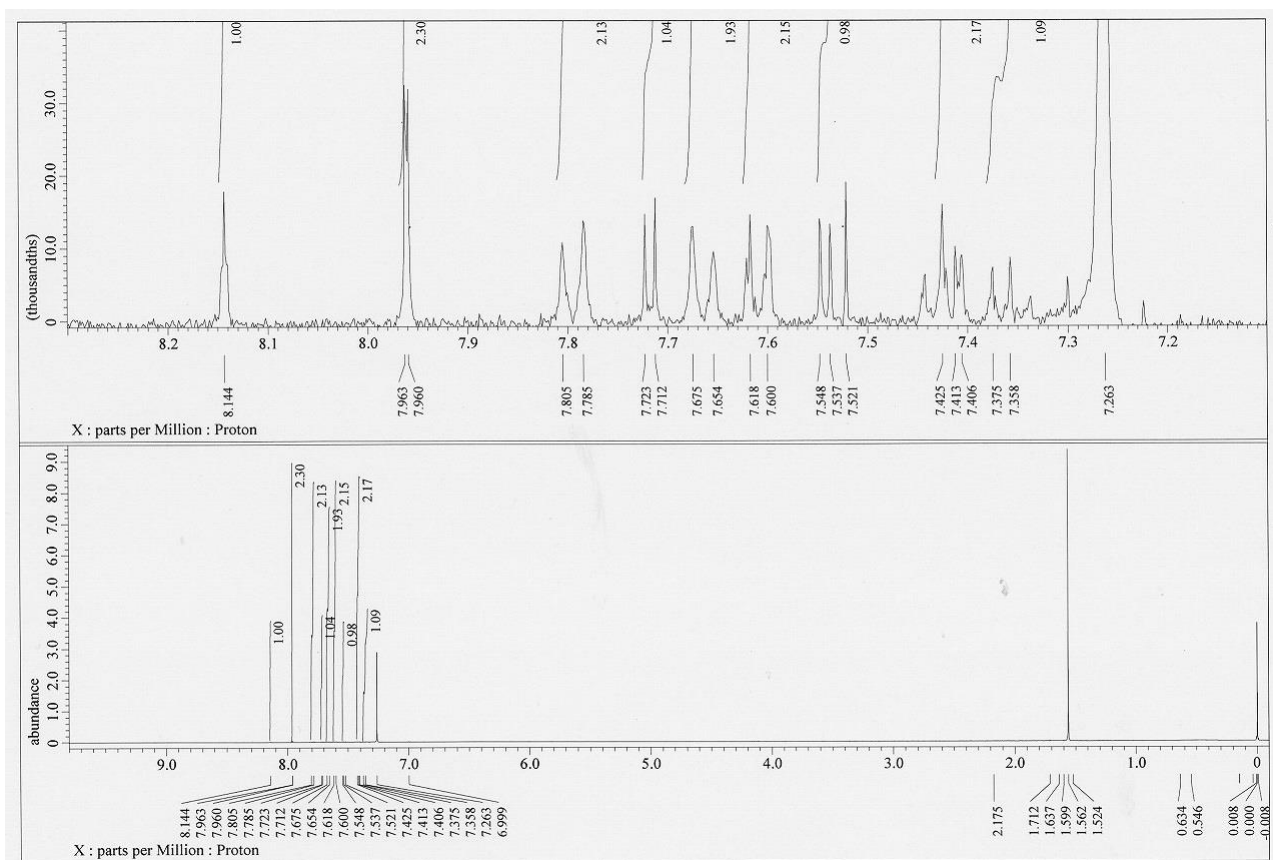


Fig. S19-4 ^1H -NMR spectrum of phenylselenophene substituted PI 4 (400 MHz).

18. ^{13}C -NMR data

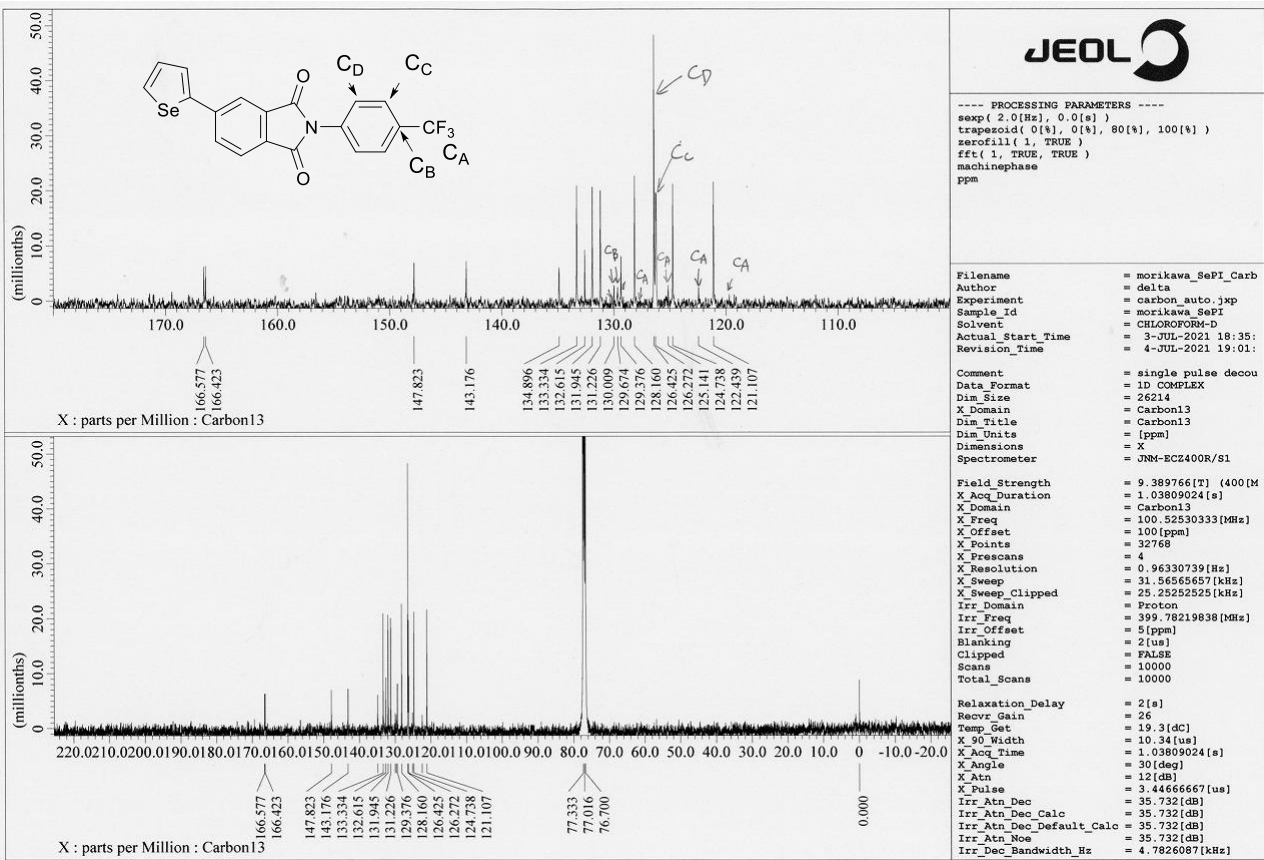


Fig. S20-1 ^{13}C -NMR spectrum of selenophene substituted PI 1 (100 MHz).

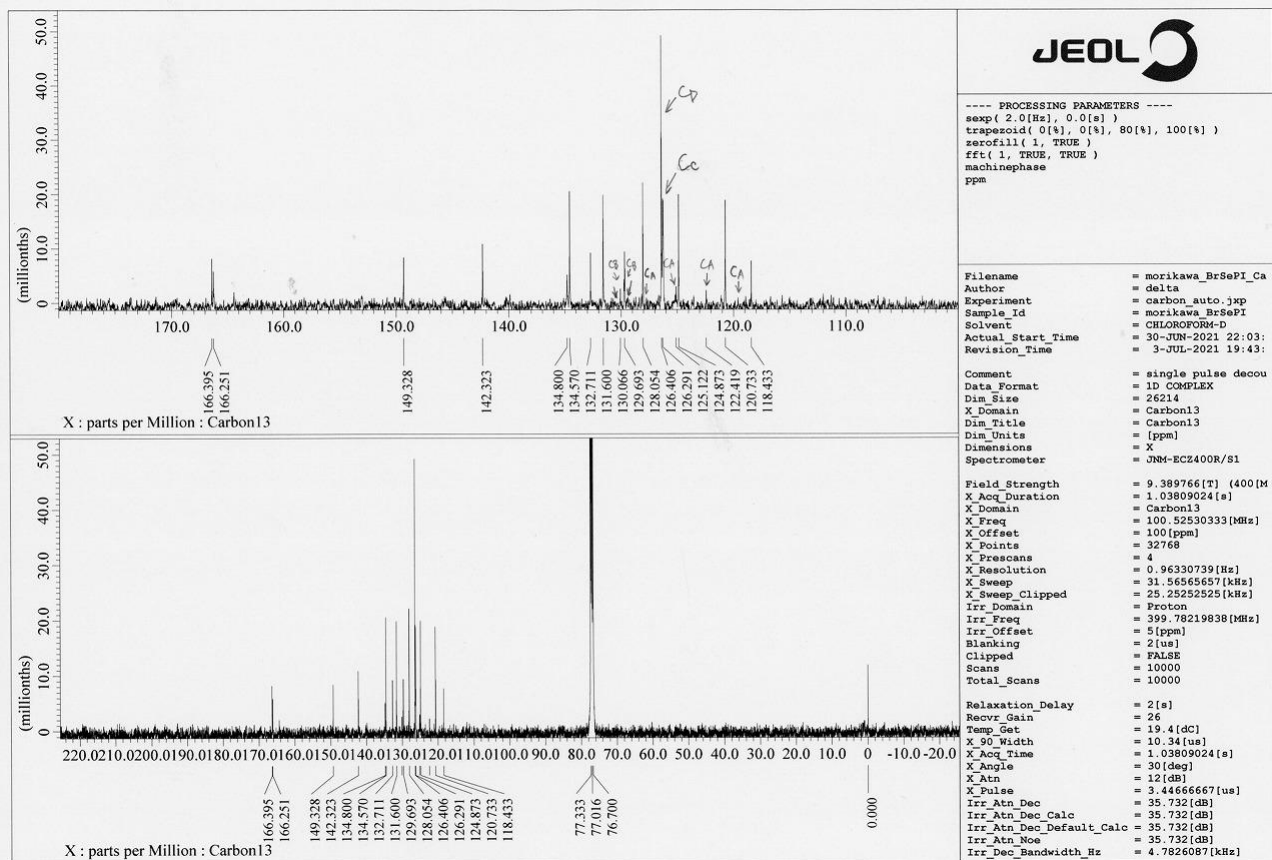


Fig. S20-2 ^{13}C -NMR spectrum of bromoselenophene substituted PI 6 (125 MHz).

21. IR data

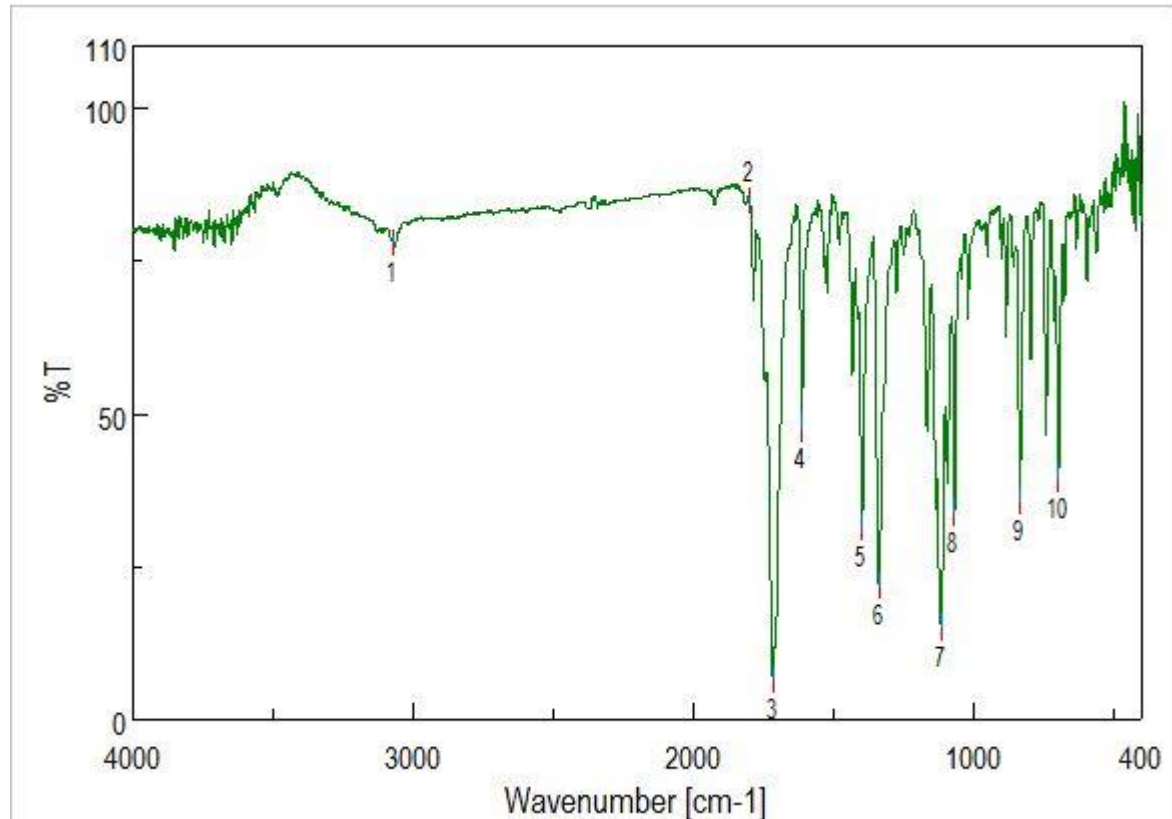


Fig. S21-1 IR spectra of selenophene substituted PI **1**.

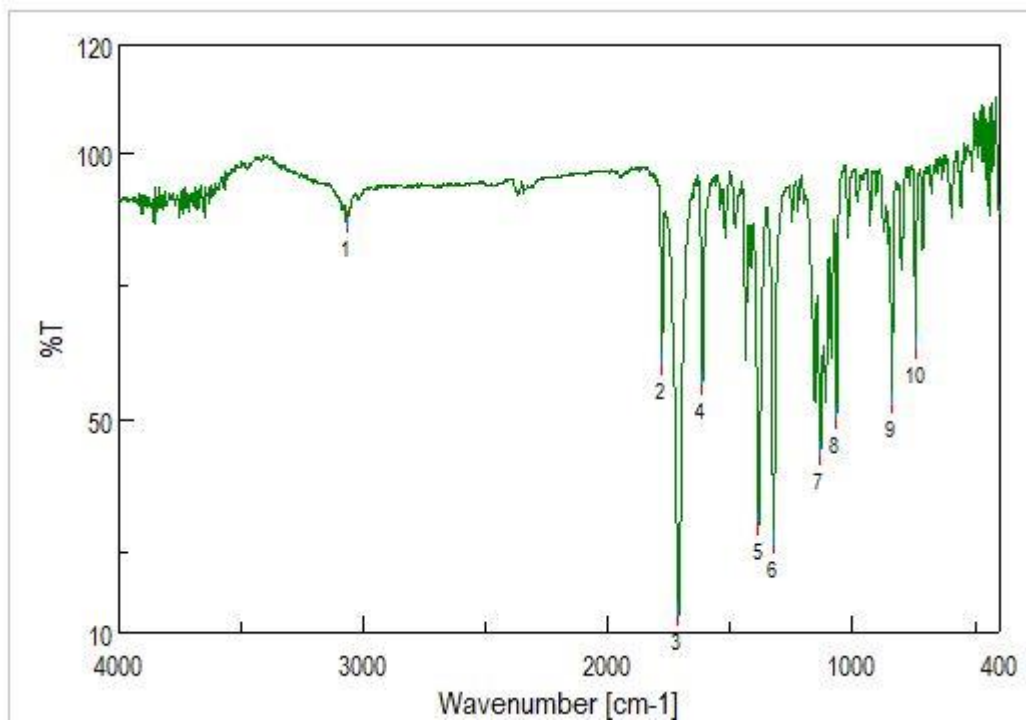


Fig. S21-2 IR spectra of bromoselenophene substituted PI **6**.

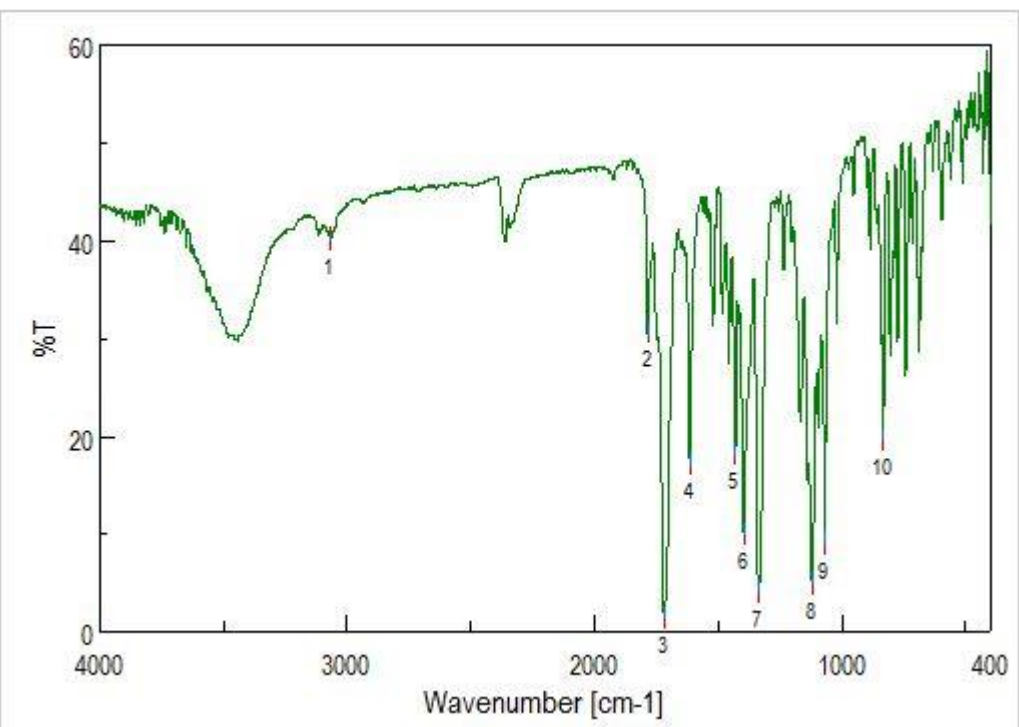


Fig. S21-3 IR spectra of biselenophene substituted PI 2.

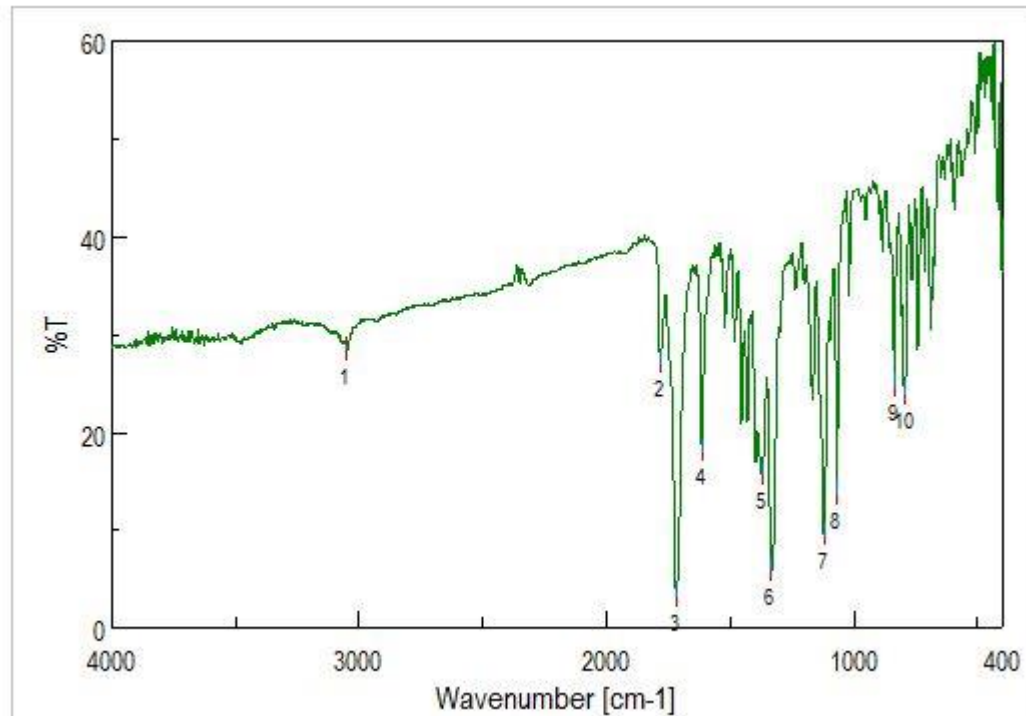


Fig. S21-4 IR spectra of terselenophene substituted PI 3.

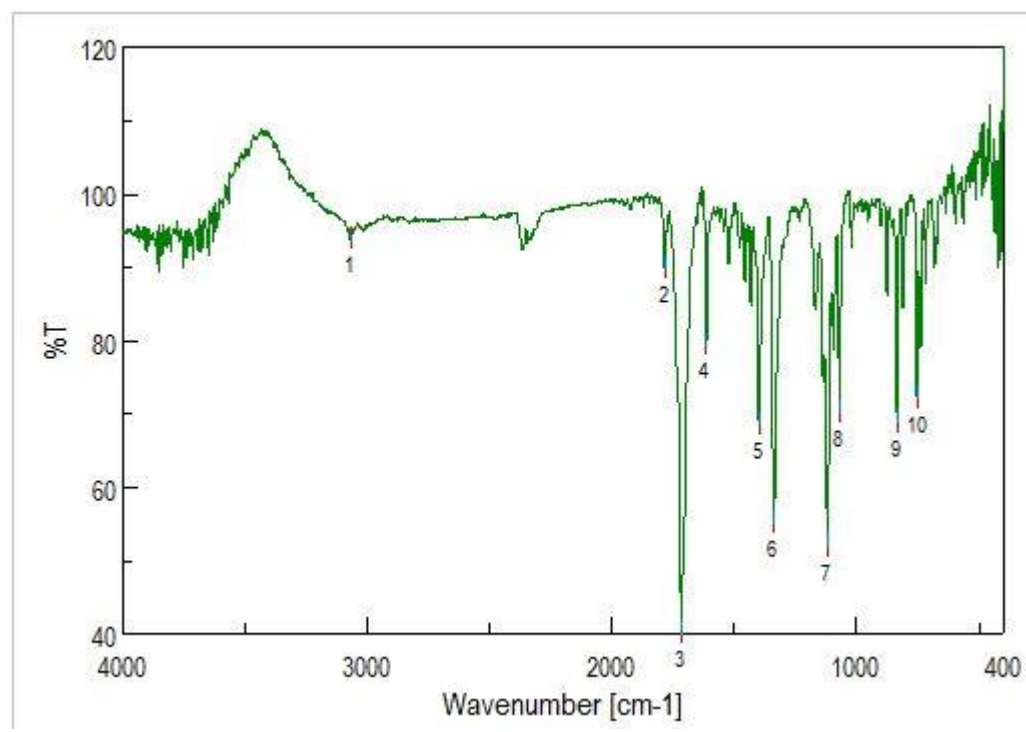


Fig. S21-5 IR spectra of phenylselenophene substituted PI 4.